ARTICLES

CCR3 is a target for age-related macular degeneration diagnosis and therapy

Atsunobu Takeda[1]*, Judit Z. Baffi[1]*, Mark E. Kleinman[1]*, Won Gil Cho[1]*, Miho Nozaki[1,3], Kiyoshi Yamada[1], Hiroki Kaneko[1], Romulo J. C. Albuquerque[1,2], Sami Dridi[1], Kuniharu Saito[1], Brian J. Raisler[1,2], Steven J. Budd[4], Pete Geisen[4], Ariel Munitz[5], Balamurali K. Ambati[6,7], Martha G. Green[1], Tatsuro Ishibashi[8], John D. Wright[4], Alison A. Humbles[9]†, Craig J. Gerard[9], Yuichiro Ogura[3], Yuzhen Pan[10], Justine R. Smith[10], Salvatore Grisanti[11], M. Elizabeth Hartnett[4], Marc E. Rothenberg[5] & Jayakrishna Ambati[1,2]

Age-related macular degeneration (AMD), a leading cause of blindness worldwide, is as prevalent as cancer in industrialized nations. Most blindness in AMD results from invasion of the retina by choroidal neovascularisation (CNV). Here we show that the eosinophil/mast cell chemokine receptor CCR3 is specifically expressed in choroidal neovascular endothelial cells in humans with AMD, and that despite the expression of its ligands eotaxin-1, -2 and -3, neither eosinophils nor mast cells are present in human CNV. Genetic or pharmacological targeting of CCR3 or eotaxins inhibited injury-induced CNV in mice. CNV suppression by CCR3 blockade was due to direct inhibition of endothelial cell proliferation, and was uncoupled from inflammation because it occurred in mice lacking eosinophils or mast cells, and was independent of macrophage and neutrophil recruitment. CCR3 blockade was more effective at reducing CNV than vascular endothelial growth factor A (VEGF-A) neutralization, which is in clinical use at present, and, unlike VEGF-A blockade, is not toxic to the mouse retina. *In vivo* imaging with CCR3-targeting quantum dots located spontaneous CNV invisible to standard fluorescein angiography in mice before retinal invasion. CCR3 targeting might reduce vision loss due to AMD through early detection and therapeutic angioinhibition.

AMD affects 30–50 million people globally, with approximately 90% of severe vision loss attributed to CNV[1]. The worldwide prevalence of CNV is expected to double in the next decade owing to population ageing. Targeting the pro-angiogenic cytokine VEGF-A has been validated in patients with CNV[2–4]. However, substantial improvement of vision only occurs in one-third of patients treated with VEGF-A antagonists, and one-sixth of treated patients still progress to legal blindness. Moreover, safety concerns about the continual blockade of VEGF-A, which is constitutively expressed in the normal adult human retina[5], are emerging[6,7]. Thus, treatment strategies on the basis of more specific targeting of CNV are desirable. However, no molecular marker specific for human CNV has yet been reported.

CCR3 expression restricted to CNV in human eyes

In our studies examining the role of chemokines in angiogenesis, we discovered that CCR3 (also known as CD193)—a chemokine receptor best known for its role in promoting eosinophil and mast cell trafficking[8]—was expressed in human choroidal endothelial cells (CECs) only in the context of CNV due to AMD, and not in other non-proliferating or proliferating choroidal vasculature (Fig. 1). Immunolocalization studies showed that CCR3 was expressed in CECs of all examined specimens of surgically excised choroidal neovascular tissue from patients with AMD (18 out of 18) who had not received prior AMD treatment (Fig. 1a, b and Supplementary Fig. 1). In contrast, CCR3 was not expressed in CECs in the choroid of any patients with early (atrophic) AMD (0 out of 10), or in age-matched patients without AMD (0 out of 10) (Fig. 1c, d). CCR3 was also not immunolocalized in surgically excised tissue from patients with epiretinal fibrotic membranes (0 out of 6), or in CECs in patients with choroidal melanoma (0 out of 8) (Fig. 1e, f). Collectively, these data point to a highly specific pattern of CCR3 expression ($P = 7 \times 10^{-14}$, exact contingency table test) in CECs in neovascular AMD. Furthermore, we identified the expression of the CCR3 ligands eotaxin-1 (also known as CCL11), -2 (CCL24), and -3 (CCL26) in all examined specimens of surgically excised choroidal neovascular tissue from patients with AMD who had not received previous AMD treatment (Fig. 1g–j), suggesting that the eotaxin–CCR3 axis could be involved in this disease state. Notably, despite the abundance of eotaxins, eosinophils and mast cells were not identified in human CNV (Supplementary Fig. 2), consistent with earlier findings[9].

CCR3 stimulation promotes CEC migration and proliferation

The best determined pathological function of CCR3 so far has been its role in allergic diseases, such as asthma[10–14] and eosinophilic esophagitis[15]. There is a single report of its direct role in angiogenesis[16]. Although eosinophils and mast cells have been reported to be

[1]Department of Ophthalmology & Visual Science, [2]Department of Physiology, University of Kentucky, Lexington, Kentucky 40506, USA. [3]Department of Ophthalmology and Visual Science, Nagoya City University Graduate School of Medical Sciences, Nagoya 467-8601, Japan. [4]Department of Ophthalmology, The University of North Carolina at Chapel Hill, Chapel Hill, North Carolina 27599, USA. [5]Division of Allergy and Immunology, Department of Pediatrics, Cincinnati Children's Hospital Medical Center, University of Cincinnati, Cincinnati, Ohio 45229, USA. [6]Department of Ophthalmology and Visual Sciences, Moran Eye Center, University of Utah School of Medicine, Salt Lake City, Utah 84132, USA. [7]Department of Ophthalmology, Veterans Affairs Salt Lake City Healthcare System, Salt Lake City, Utah 84148, USA. [8]Department of Ophthalmology, Graduate School of Medical Sciences, Kyushu University, Fukuoka 812-8582, Japan. [9]Department of Medicine, Children's Hospital, Harvard Medical School, Boston, Massachusetts 02215, USA. [10]Casey Eye Institute, Oregon Health and Science University, Portland, Oregon 97239, USA. [11]Department of Ophthalmology, University of Luebeck, D-23538 Lübeck, Germany. †Present address: Respiratory, Inflammation and Autoimmunity, Medimmune, Inc., Gaithersburg, Maryland 20878, USA.
*These authors contributed equally to this work.

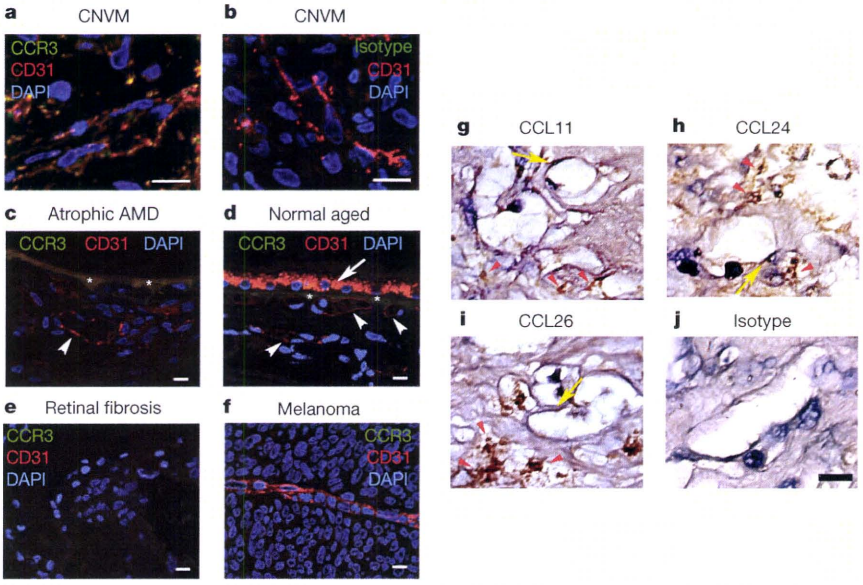

Figure 1 | CCR3 and eotaxins are expressed in CNV. **a**, **b**, Immunofluorescence shows that CCR3-receptor expression (green) colocalizes with $CD31^+$-expressing (red) blood vessels in surgically excised human AMD choroidal neovascular tissue (CNVM). Nuclei were stained blue with 4,6-diamidino-2-phenylindole (DAPI). The specificity of CCR3 staining in **a** is confirmed by the absence of staining with an isotype control IgG (green) in **b**. Individual red and green fluorescence channels are shown in Supplementary Fig. 1. **c**, **d**, CCR3 is not immunolocalized in $CD31^+$ (red) blood vessels (white arrowheads) in the choroid of patients with atrophic AMD who do not have CNV (**c**), or in aged patients without AMD (**d**). Autofluorescence of RPE (white arrow) and Bruch's membrane (asterisks) overlying choroid are seen. **e**, **f**, CCR3 is not expressed in surgically excised avascular retinal fibrosis tissue (**e**) or in the blood vessel of choroidal melanoma (**f**). **g–j**, Immunohistochemistry (golden brown reaction product) shows expression of CCL11 (**g**), CCL24 (**h**), and CCL26 (**i**) in surgically excised AMD choroidal neovascular tissue, primarily in the stroma (red arrowheads) but also in the blood vessels (yellow arrows). The specificity of staining is confirmed by the absence of staining with isotype control IgG (**j**). Scale bars, 10 μm.

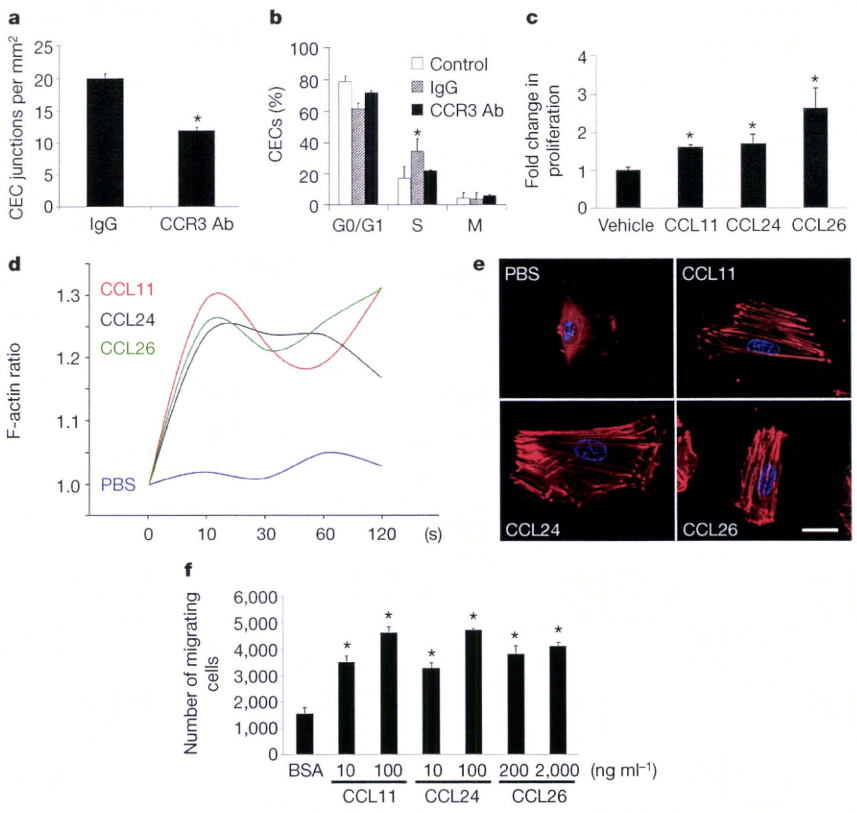

Figure 2 | CCR3 activation promotes angiogenesis. **a**, Tube formation of primary human CECs in Matrigel *in vitro* was reduced by neutralizing anti-human CCR3 antibodies (CCR3 Ab) compared to isotype IgG. $n = 6$, $^*P < 0.05$ compared to isotype IgG. **b**, Fraction of $CD31^+VEGFR2^+$-gated mouse CECs *in vivo* in the proliferative state (S phase) was increased 5 days after laser injury in wild-type mouse eyes compared to control (uninjured eyes), and was reduced by intraocular administration of neutralizing anti-mouse CCR3 antibody compared to isotype IgG. $n = 6$–10, $^*P < 0.05$ compared to IgG treatment. **c**, Stimulation with eotaxins for 24 h induced human CEC proliferation. $n = 4$, $^*P < 0.05$ compared to BSA treatment. **d**, **e**, Stimulation with eotaxins, but not with PBS, induced actin polymerization in human CECs. The relative F-actin content is expressed as the ratio of the mean channel fluorescence between eotaxin-stimulated and media-alone-stimulated cells (**d**). Rhodamine–phalloidin staining (red) shows F-actin fibre formation in eotaxin-stimulated cells (**e**). Nuclei were stained blue with DAPI. Data representative of 3–4 independent experiments are shown. In **c** and **e**, 10 ng ml^{-1} CCL11, 100 ng ml^{-1} CCL24 and 2 μg ml^{-1} CCL26 were used. Scale bar, 20 μm. **f**, Stimulation with eotaxins for 16 h induces dose-dependent migration of human CECs across 8-μm pore size Transwells. $n = 5$–10, $^*P < 0.05$ compared to BSA treatment. Statistical significance was determined by Mann–Whitney U test (**a–c**, **f**); error bars depict s.e.m.

involved in angiogenesis[17,18], such actions are considered minor or isolated. Therefore, we studied the effects of CCR3 modulation on angiogenesis *in vitro* and *in vivo*. Neutralizing anti-CCR3 antibodies inhibited the tube formation of primary human CECs cultured in Matrigel *in vitro* (Fig. 2a). In an experimental model of CNV induced by laser injury in wild-type mice[19–24], neutralizing anti-CCR3 antibodies reduced the fraction of CECs *in vivo* that was in the proliferative state of the cell cycle (Fig. 2b). Consistent with this finding, each of the three eotaxins stimulated human CEC proliferation (Fig. 2c). Cytoskeletal rearrangement through polymerization of monomeric actin to microfilamentous F-actin, which is essential for eosinophil chemotaxis induced by the eotaxins, is also critical in angiogenic migration of endothelial cells. Stimulation of human CECs with any of the three eotaxins induced a rapid polymerization of actin molecules (Fig. 2d, e). All three eotaxins also activated RAC1 (Supplementary Fig. 3), a small GTPase that is critical in regulating endothelial cell spreading and migration, and promoted human CEC migration in a dose-dependent fashion (Fig. 2f). Collectively, these data demonstrate that CCR3 activation can promote several steps of angiogenesis. The expression of CCR3 on CECs *in vivo* is confined to choroidal neovascular tissues; however, *in vitro*, human CECs responded to CCR3 ligands. This might be owing to the presence of several CNV-promoting growth factors in the culture medium.

CCR3 receptor or ligand antagonism inhibits CNV

We studied the *in vivo* effects of CCR3 targeting in a mouse model of CNV induced by laser injury[22], which is the most widely used animal model of this disease. A single intraocular administration of either CCR3-neutralizing antibodies or a small molecule CCR3 receptor antagonist ((*S*)-methyl-2-naphthoylamino-3-(4-nitrophenyl)propionate; SB328437) suppressed laser-injury-induced CNV in wild-type mice in a dose-dependent fashion (Fig. 3a–c). CNV was also diminished in $Ccr3^{-/-}$ mice[25] compared to wild-type mice (Fig. 3d). The specificity of pharmacological CCR3 blockade was confirmed by demonstrating that CNV was not reduced in $Ccr3^{-/-}$ mice by CCR3-neutralizing antibodies or a CCR3 receptor antagonist (116 ± 7% and 109 ± 16% of control, respectively; $n = 5$; $P > 0.1$). CCL11 and CCL24, the principal mouse ligands for CCR3, were markedly increased soon after laser injury, and immunolocalized to the retinal pigmented epithelium (RPE), which is adjacent to CECs (Fig. 3e, f).

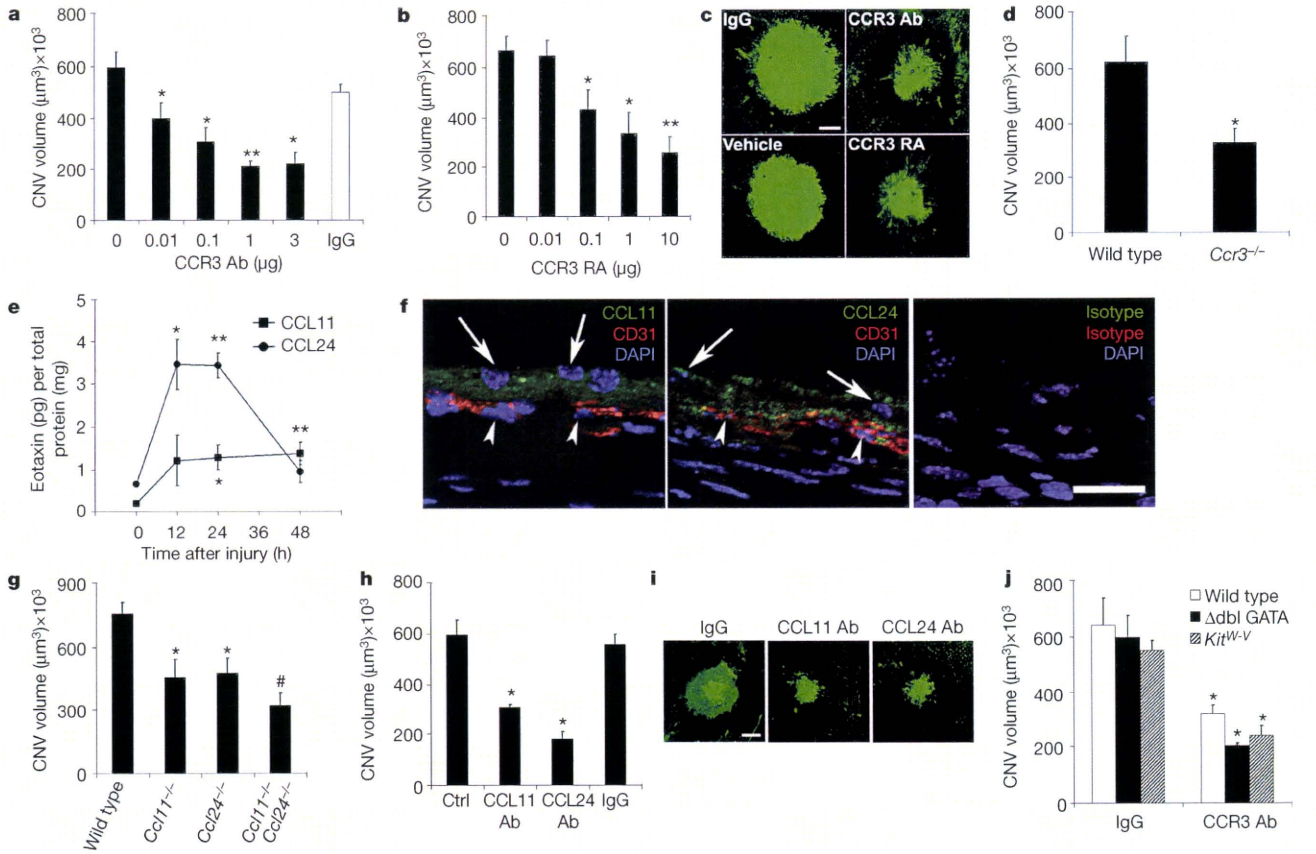

Figure 3 | CNV reduced by CCR3 or eotaxin ablation or blockade independent of leukocyte modulation. a, b, Laser-induced CNV in wild-type mice was reduced by neutralizing anti-mouse CCR3 antibody (CCR3 Ab) compared to isotype IgG (**a**) and by the CCR3 receptor antagonist (RA) SB328437 compared to vehicle (PBS/DMSO) (**b**) in a dose-dependent fashion. $n = 8$–12, $^*P < 0.05$, $^{**}P < 0.01$ compared to no antibody or receptor antagonist. **c**, Representative examples of CNV in drug-treated mice. **d**, Laser-induced CNV was reduced in $Ccr3^{-/-}$ mice compared to wild-type mice. $n = 9$, $^*P < 0.05$ compared to wild-type mice. **e**, Eotaxin-1 (CCL11) and eotaxin-2 (CCL24) protein levels, measured by ELISA, were increased after laser injury in wild-type mice. $n = 6$, $^*P < 0.05$ and $^{**}P < 0.01$ compared to the 0 h baseline. **f**, CCL11 and CCL24 immunofluorescence (green) was localized in the RPE cell layer (arrows) adjacent to $CD31^+$ (red) CECs (arrowheads) on day 1 after laser injury in wild-type mice. Nuclei were stained blue by DAPI. No specific immunofluorescence was detected with isotype control IgGs. Images representative of three independent experiments are shown. **g**, Laser-induced CNV was reduced in $Ccl11^{-/-}$ and $Ccl24^{-/-}$ mice compared to wild-type mice. $n = 8$–10, $^*P < 0.05$ compared to wild-type mice. CNV is further reduced in $Ccl11^{-/-}$ $Ccl24^{-/-}$ mice compared to single-null mice. $\#P < 0.05$ compared to single-null mice. **h**, Laser-induced CNV in wild-type mice was reduced by neutralizing antibodies against mouse CCL11 or CCL24 compared to isotype IgG. $n = 7$–10, $^*P < 0.05$ compared to no injection (control; Ctrl) or IgG. **i**, Representative examples of CNV in eotaxin-neutralized mice. **j**, Neutralizing anti-CCR3 antibodies reduced laser-induced CNV in mice deficient in eosinophils (Δdbl GATA) or mast cells ($Kit^{W\text{-}v}$). $n = 6$–9, $^*P < 0.05$ compared to IgG. Scale bars, 100 μm (**c**, **i**), and 20 μm (**f**). Error bars depict s.e.m.

Also, human RPE cells synthesized all three eotaxins (Supplementary Fig. 4), implicating these cells, which are abundantly interspersed in CNV[9], as a source of CCR3 ligands in CNV. Genetic ablation of either *Ccl11* (ref. 26) or *Ccl24* (ref. 12) reduced CNV, whereas the neovascular response in *Ccl11*$^{-/-}$ *Ccl24*$^{-/-}$ mice[12] was suppressed to a greater extent than in either of the single knockout mice, suggesting cooperation between these two ligands in this system (Fig. 3g). A single intraocular administration of neutralizing antibodies against CCL11 or CCL24 also suppressed CNV in wild-type mice (Fig. 3h, i), validating these CCR3 ligands as anti-angiogenic targets. Together, these data demonstrate that CCR3 activation is essential for *in vivo* angiogenesis in the most widely used preclinical model of neovascular AMD.

CCR3-driven angiogenesis uncoupled from inflammation

We sought to determine whether CCR3 targeting reduced CNV solely by anti-angiogenic mechanisms, or whether anti-inflammatory mechanisms were also involved. Neither eosinophils nor mast cells (defined as CCR3^{hi}CD3^{-}CD117^{int}CD49d^{+} and CCR3^{int}CD3^{-}CD117^{hi}CD49d^{+} cells, respectively) were recruited to the choroid after laser injury, as monitored by flow cytometry (Supplementary Fig. 5). Furthermore, the CNV response in eosinophil-deficient ΔdblGATA mice[11] (containing a deletion of the double GATA site) and mast-cell-deficient *Kit*$^{W\text{-}v}$/*Kit*$^{W\text{-}v}$ mice[27] was not different from the response in wild-type mice (Fig. 3j). Moreover, intraocular administration of neutralizing anti-CCR3 antibodies reduced CNV in ΔdblGATA or *Kit*$^{W\text{-}v}$/*Kit*$^{W\text{-}v}$ mice to the same extent as in wild-type mice. Thus, although eosinophils and mast cells have been reported to be capable of driving angiogenesis in other systems[17,18], both cell types are dispensable in the development of experimental CNV. Although neutrophil and macrophage infiltration are crucial for the development of experimental CNV[23,28], CCR3-receptor targeting did not affect recruitment of either inflammatory cell type (defined as Gr-1^{+}F4/80^{-} and F4/80^{+}CD11c^{-} cells, respectively; Supplementary Fig. 5). Therefore, the angioinhibitory effect of CCR3 blockade in this model is a direct anti-vascular effect, and does not seem to involve modulation of cellular inflammation. The mechanisms underlying the paucity of eosinophils and mast cells in CNV remain to be defined. One potential explanation could be the expression of CXCL9 in CNV, which blocks eotaxin-induced CCR3-mediated eosinophil recruitment (Supplementary Fig. 6)[29,30]. Other mechanisms influencing adhesion or mobilization of these leukocytes might also be operative.

CNV bioimaging by CCR3 targeting

Because invasion of the retina by CNV results in morphological and functional disruption of the retina, early detection of CNV is desirable; indeed, detection of CNV before retinal invasion would be ideal. CNV that has breached the retina can be detected by fluorescein angiography. However, this diagnostic modality cannot detect CNV before it has invaded the retina, that is, when it is still limited to the choroid. Yet, post-mortem histopathological studies have shown that substantial numbers of patients in whom fluorescein angiography does not reveal the presence of CNV nevertheless have CNV that has not yet invaded the retina[31]. Therefore, we explored whether CCR3-targeted bioimaging using anti-CCR3 Fab antibody fragments (Supplementary Fig. 7) conjugated to quantum dots (QDot-CCR3 Fab) could detect CNV before it became clinically evident.

We previously described the spontaneous development of CNV in senescent mice deficient in monocyte chemoattractant protein-1 (CCL2, also known as MCP-1) or its CCR2 receptor[32]. Similar pathology occurs at a younger age in *Ccl2*$^{-/-}$ *Ccr2*$^{-/-}$ mice (J.A., M.E.K., J.Z.B., H.K. and B.J.R., unpublished data). These mice also undergo outer retinal degeneration rapidly (Supplementary Fig. 8). We tested whether fundus angiography after intravenous injection of QDot-CCR3 Fab could detect subretinal CNV in these mice. QDot-CCR3 Fab angiography demonstrated hyperfluorescent signals in regions of the fundus of these mice that were silent on fluorescein angiography (Fig. 4a, b). The specificity of CCR3 targeting was confirmed by the absence of hyperfluorescent signals in *Ccl2*$^{-/-}$ *Ccr2*$^{-/-}$ mice injected with QDot-isotype Fab, and in wild-type mice injected with QDot-CCR3 Fab (Fig. 4b and Supplementary Fig. 9). Histological examination of these areas showed proliferating (Ki67^{+}) CCR3^{+} blood vessels in the choroid that had not yet invaded the retina, along with the accumulation of QDot-CCR3 Fab in these vessels (Fig. 4c–g). These data provide proof-of-principle that CCR3-targeted bioimaging can detect subclinical CNV before it disrupts the retina and causes vision loss.

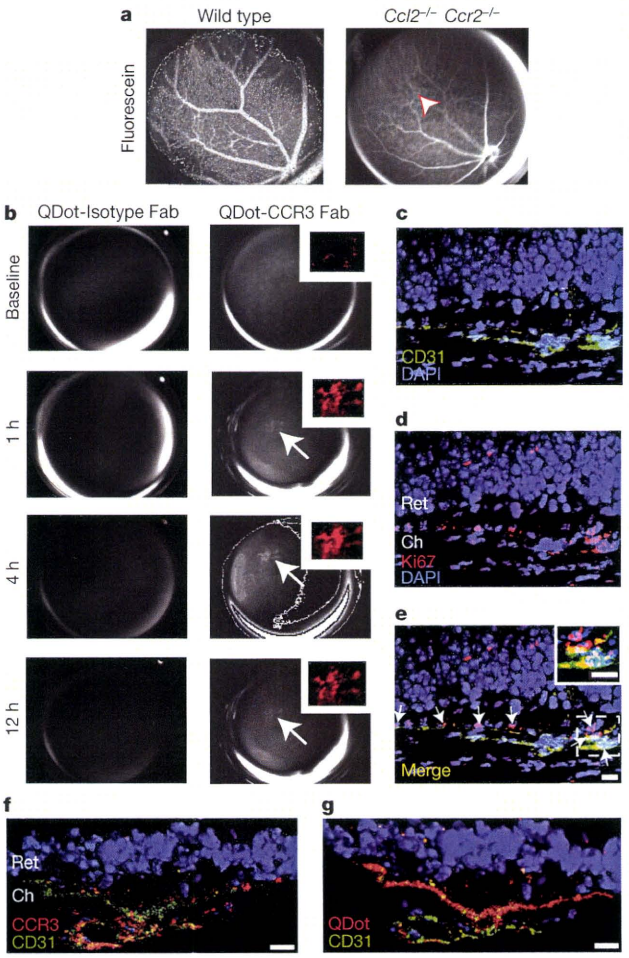

Figure 4 | CCR3-targeting quantum dots detect subretinal CNV. a, Images of the fundus taken after intravenous injection of sodium fluorescein in wild-type and *Ccl2*$^{-/-}$ *Ccr2*$^{-/-}$ mice show normal retinal vascular filling but no areas of hyperfluorescence indicative of CNV. **b**, After intravenous injection of QDot-CCR3 Fab in the same *Ccl2*$^{-/-}$ *Ccr2*$^{-/-}$ mouse shown in **a**, focal branching choroidal hyperfluorescence was visualized (arrow) at 1 h in the same area that was not hyperfluorescent during fluorescein angiography (arrowhead in **a**). The intensity of this hyperfluorescence (shown in red pseudocolour in the inset) increased, attaining a peak at 4 h, and then declined in intensity but still persisted at 12 h. Corresponding images of QDot-Isotype Fab angiography showed no hyperfluorescence. **c–e**, The region corresponding to the area of hyperfluorescence seen on QDot-CCR3 Fab angiography in **b** contained several CD31^{+} blood vessels in the choroid (Ch) that were proliferating (Ki67^{+}; arrows) and had not invaded the retina (Ret). Individual green (CD31^{+}, **c**), red (Ki67^{+}, **d**), and merged (**e**) fluorescence channel images are shown. Nuclei were stained with DAPI (blue). Arrows point to proliferating endothelial cells. The inset in **e** shows Ki67^{+} CD31^{+} cells in higher magnification. **f**, QDot-CCR3 Fab hyperfluorescent areas were localized to areas of subretinal CNV with CCR3^{+} endothelial cells. **g**, The QDot label was visualized within CD31^{+} vasculature of subretinal CNV lesions. Images are representative of six independent experiments. Scale bars, 10 μm (**c–g**).

CCR3 targeting is superior to VEGF-A targeting

By comparing CCR3 targeting to VEGF-A targeting, the most effective approved treatment for human CNV, we found that CCR3-neutralizing antibodies were more effective than VEGF-A-neutralizing antibodies (68 ± 3% versus 57 ± 4%) at inhibiting laser-induced CNV in mice (Supplementary Fig. 10). In the laser-injury model, CCR3 neutralization did not change VEGF-A levels in the RPE/choroid and VEGF-A blockade did not change CCR3 expression on CECs (Supplementary Fig. 11): these two pathways seem to not be directly coupled. Repeated intravitreous administration of anti-VEGF-A antibodies resulted in anatomical and functional damage to the retina in wild-type mice (Supplementary Fig. 12), consistent with earlier reports that anti-VEGF-A therapy induces dysfunction in and damage to the inner and outer murine retina[6,7]. These effects were modest at a dose of anti-VEGF-A antibodies that suppressed mouse CNV, but more pronounced at a higher dose that is comparable to the dose used in humans. It should be noted that anti-VEGF-A pharmacotherapy has not been associated with an increased risk of profound retinal damage in humans[33], but subtle abnormalities have been observed[34,35] and some adverse effects might be misattributed to disease progression. In contrast to VEGF-A blockade, neither an anti-CCR3 antibody nor a CCR3 receptor antagonist induced retinal toxicity in wild-type mice, as confirmed by fundus imaging and electrophysiological function (Supplementary Fig. 12). *Vegfa* deletion is embryonically lethal[36,37] and conditional ablation of *Vegfa* in the RPE induces profound retinal degeneration and visual dysfunction[38]. In contrast, the $Ccr3^{-/-}$ mouse retina was normal in appearance and electrophysiological function (Supplementary Fig. 13).

Discussion

Our findings suggest that CCR3 targeting may be a safe and viable strategy for early detection (using biocompatible quantum dots or other bioimaging fluorochromes, such as near infrared dyes) and treatment of CNV (by receptor or ligand targeting), and might be superior to the current standard of care. CCR3 bioimaging is probably most useful in individuals with RPE pigmentary disturbances and multiple subretinal lipoproteinaceous deposits known as drusen or fellow eye involvement with clinically evident CNV, as they are known to be at high risk for developing CNV[39,40]. Similar techniques might be useful in non-invasively bioimaging other metabolic or molecular markers to provide information about disease pathogenesis or activity.

Several strategies have yielded molecular markers that are preferentially expressed on proliferating endothelial cells such as those in tumour vasculature[41,42]; however, CCR3 has not been identified in any of these reports. Therefore, our studies identify CCR3 as a new marker of pathological angiogenesis and as a functional target in neovascular AMD. These findings should also prompt a search for genetic polymorphisms in the eotaxin–CCR3 axis in patients with AMD, and investigations of CCR3 function in other models of angiogenesis. Also, it is tempting to speculate that targeting CCR3 might provide dual benefits in asthma, which involves varying degrees of eosinophilic inflammation as well as angiogenic airway remodelling[43].

METHODS SUMMARY

Mouse model of CNV. Laser photocoagulation (OcuLight GL, Iridex Corporation) was performed on mouse eyes to induce CNV, and CNV volumes were measured 7 days after injury by scanning laser confocal microscopy (TCS SP, Leica), as previously described[22].

Drug injections. Rat IgG2a neutralizing antibody against mouse CCR3 (R&D Systems), control rat IgG2a (Serotec), goat neutralizing antibody against mouse CCL11 (R&D Systems), goat neutralizing antibody against mouse CCL24 (R&D Systems), control goat IgG (Jackson Immunoresearch), or (*S*)-methyl-2-naphthoylamino-3-(4-nitrophenyl)propionate (SB328437; Calbiochem) dissolved in dimethylsulphoxide (DMSO) were injected into the vitreous humour using a 33-gauge double-calibre needle (Ito Corporation) once, immediately after laser injury as previously described[22].

CCR3 bioimaging. Fab fragments were created from monoclonal IgG2a antibody raised against the extracellular domain of murine CCR3 (R&D Systems) and an isotype rat IgG2a (R&D Systems) using a commercially available papain-based kit (Pierce). Recovered fragments were conjugated with quantum dots (Invitrogen, QDot-800) and resuspended in sterile PBS. $Ccl2^{-/-}$ $Ccr2^{-/-}$ mice were administered 100 μg of tagged CCR3 Fab or isotype Fab by tail-vein injection after acquiring baseline fluorescent imaging using a Topcon retinal camera (TRC-50IX). Serial images were then acquired at 1, 4 and 12 h, after which eyes were collected and frozen in OCT for immunofluorescent analyses. Retinal images were analysed (ImageNet, Topcon) by comparison to baseline and fluorescein angiographic data. Hyperfluorescent areas were then cropped, equally thresholded, and pseudocoloured (Photoshop CS3, Adobe). Sections from QDot-conjugated CCR3 or rat IgG2a isotype Fab injected animals were fixed in 4% paraformaldehyde and blocked with 5% normal donkey serum/5% goat serum in PBS, stained with rat anti-mouse CD31 (BD Biosciences) and either rabbit anti-mouse CCR3 (Santa Cruz) or rabbit anti-Ki67 (Abcam), followed by appropriate fluorescent secondary antibodies (Alexa Fluor 488/594, Invitrogen), and evaluated by confocal laser scanning microscopy (Leica SP-5).

Full Methods and any associated references are available in the online version of the paper at www.nature.com/nature.

Received 22 March; accepted 21 May 2009.
Published online 14 June 2009.

1. Ambati, J., Ambati, B. K., Yoo, S. H., Ianchulev, S. & Adamis, A. P. Age-related macular degeneration: etiology, pathogenesis, and therapeutic strategies. *Surv. Ophthalmol.* **48**, 257–293 (2003).
2. Gragoudas, E. S., Adamis, A. P., Cunningham, E. T. Jr, Feinsod, M. & Guyer, D. R. Pegaptanib for neovascular age-related macular degeneration. *N. Engl. J. Med.* **351**, 2805–2816 (2004).
3. Brown, D. M. *et al.* Ranibizumab versus verteporfin for neovascular age-related macular degeneration. *N. Engl. J. Med.* **355**, 1432–1444 (2006).
4. Rosenfeld, P. J. *et al.* Ranibizumab for neovascular age-related macular degeneration. *N. Engl. J. Med.* **355**, 1419–1431 (2006).
5. Famiglietti, E. V. *et al.* Immunocytochemical localization of vascular endothelial growth factor in neurons and glial cells of human retina. *Brain Res.* **969**, 195–204 (2003).
6. Nishijima, K. *et al.* Vascular endothelial growth factor-A is a survival factor for retinal neurons and a critical neuroprotectant during the adaptive response to ischemic injury. *Am. J. Pathol.* **171**, 53–67 (2007).
7. Saint-Geniez, M. *et al.* Endogenous VEGF is required for visual function: evidence for a survival role on muller cells and photoreceptors. *PLoS One* **3**, e3554 (2008).
8. Rothenberg, M. E. & Hogan, S. P. The eosinophil. *Annu. Rev. Immunol.* **24**, 147–174 (2006).
9. Submacular Surgery Trials Research Group. Histopathologic and ultrastructural features of surgically excised subfoveal choroidal neovascular lesions: submacular surgery trials report no. 7. *Arch. Ophthalmol.* **123**, 914–921 (2005).
10. Justice, J. P. *et al.* Ablation of eosinophils leads to a reduction of allergen-induced pulmonary pathology. *Am. J. Physiol. Lung Cell. Mol. Physiol.* **284**, L169–L178 (2003).
11. Humbles, A. A. *et al.* A critical role for eosinophils in allergic airways remodeling. *Science* **305**, 1776–1779 (2004).
12. Pope, S. M., Zimmermann, N., Stringer, K. F., Karow, M. L. & Rothenberg, M. E. The eotaxin chemokines and CCR3 are fundamental regulators of allergen-induced pulmonary eosinophilia. *J. Immunol.* **175**, 5341–5350 (2005).
13. Jose, P. J. *et al.* Eotaxin: a potent eosinophil chemoattractant cytokine detected in a guinea pig model of allergic airways inflammation. *J. Exp. Med.* **179**, 881–887 (1994).
14. Teixeira, M. M. *et al.* Chemokine-induced eosinophil recruitment. Evidence of a role for endogenous eotaxin in an *in vivo* allergy model in mouse skin. *J. Clin. Invest.* **100**, 1657–1666 (1997).
15. Blanchard, C. *et al.* Eotaxin-3 and a uniquely conserved gene-expression profile in eosinophilic esophagitis. *J. Clin. Invest.* **116**, 536–547 (2006).
16. Salcedo, R. *et al.* Eotaxin (CCL11) induces *in vivo* angiogenic responses by human $CCR3^+$ endothelial cells. *J. Immunol.* **166**, 7571–7578 (2001).
17. Puxeddu, I. *et al.* Human peripheral blood eosinophils induce angiogenesis. *Int. J. Biochem. Cell Biol.* **37**, 628–636 (2005).
18. Heissig, B. *et al.* Low-dose irradiation promotes tissue revascularization through VEGF release from mast cells and MMP-9-mediated progenitor cell mobilization. *J. Exp. Med.* **202**, 739–750 (2005).
19. Tobe, T. *et al.* Targeted disruption of the FGF2 gene does not prevent choroidal neovascularization in a murine model. *Am. J. Pathol.* **153**, 1641–1646 (1998).
20. Nozaki, M. *et al.* Drusen complement components C3a and C5a promote choroidal neovascularization. *Proc. Natl Acad. Sci. USA* **103**, 2328–2333 (2006).
21. Nozaki, M. *et al.* Loss of SPARC-mediated VEGFR-1 suppression after injury reveals a novel antiangiogenic activity of VEGF-A. *J. Clin. Invest.* **116**, 422–429 (2006).
22. Kleinman, M. E. *et al.* Sequence- and target-independent angiogenesis suppression by siRNA via TLR3. *Nature* **452**, 591–597 (2008).

23. Sakurai, E., Anand, A., Ambati, B. K., van Rooijen, N. & Ambati, J. Macrophage depletion inhibits experimental choroidal neovascularization. *Invest. Ophthalmol. Vis. Sci.* **44,** 3578–3585 (2003).
24. Sakurai, E. *et al.* Targeted disruption of the CD18 or ICAM-1 gene inhibits choroidal neovascularization. *Invest. Ophthalmol. Vis. Sci.* **44,** 2743–2749 (2003).
25. Humbles, A. A. *et al.* The murine CCR3 receptor regulates both the role of eosinophils and mast cells in allergen-induced airway inflammation and hyperresponsiveness. *Proc. Natl Acad. Sci. USA* **99,** 1479–1484 (2002).
26. Rothenberg, M. E., MacLean, J. A., Pearlman, E., Luster, A. D. & Leder, P. Targeted disruption of the chemokine eotaxin partially reduces antigen-induced tissue eosinophilia. *J. Exp. Med.* **185,** 785–790 (1997).
27. Kitamura, Y., Go, S. & Hatanaka, K. Decrease of mast cells in *W/W*^{v} mice and their increase by bone marrow transplantation. *Blood* **52,** 447–452 (1978).
28. Zhou, J. *et al.* Neutrophils promote experimental choroidal neovascularization. *Mol. Vis.* **11,** 414–424 (2005).
29. Fulkerson, P. C. *et al.* Negative regulation of eosinophil recruitment to the lung by the chemokine monokine induced by IFN-γ (Mig, CXCL9). *Proc. Natl Acad. Sci. USA* **101,** 1987–1992 (2004).
30. Fulkerson, P. C., Zhu, H., Williams, D. A., Zimmermann, N. & Rothenberg, M. E. CXCL9 inhibits eosinophil responses by a CCR3- and Rac2-dependent mechanism. *Blood* **106,** 436–443 (2005).
31. Green, W. R. & Key, S. N. III. Senile macular degeneration: a histopathologic study. *Trans. Am. Ophthalmol. Soc.* **75,** 180–254 (1977).
32. Ambati, J. *et al.* An animal model of age-related macular degeneration in senescent Ccl-2- or Ccr-2-deficient mice. *Nature Med.* **9,** 1390–1397 (2003).
33. Ip, M. S. *et al.* Anti-vascular endothelial growth factor pharmacotherapy for age-related macular degeneration: a report by the American Academy of Ophthalmology. *Ophthalmology* **115,** 1837–1846 (2008).
34. Sayanagi, K., Sharma, S. & Kaiser, P. K. Photoreceptor status after anti-vascular endothelial growth factor therapy in exudative age-related macular degeneration. *Br. J. Ophthalmol.* **93,** 622–626 (2009).
35. Yodoi, Y. *et al.* Central retinal sensitivity after intravitreal injection of bevacizumab for myopic choroidal neovascularization. *Am. J. Ophthalmol.* **147,** 816–824 (2009).
36. Carmeliet, P. *et al.* Abnormal blood vessel development and lethality in embryos lacking a single VEGF allele. *Nature* **380,** 435–439 (1996).
37. Ferrara, N. *et al.* Heterozygous embryonic lethality induced by targeted inactivation of the VEGF gene. *Nature* **380,** 439–442 (1996).
38. Marneros, A. G. *et al.* Vascular endothelial growth factor expression in the retinal pigment epithelium is essential for choriocapillaris development and visual function. *Am. J. Pathol.* **167,** 1451–1459 (2005).
39. Bressler, S. B., Maguire, M. G., Bressler, N. M. & Fine, S. L. (The Macular Photocoagulation Study Group). Relationship of drusen and abnormalities of the retinal pigment epithelium to the prognosis of neovascular macular degeneration. *Arch. Ophthalmol.* **108,** 1442–1447 (1990).
40. Macular Photocoagulation Study Group. Risk factors for choroidal neovascularization in the second eye of patients with juxtafoveal or subfoveal choroidal neovascularization secondary to age-related macular degeneration. *Arch. Ophthalmol.* **115,** 741–747 (1997).
41. St Croix, B. *et al.* Genes expressed in human tumor endothelium. *Science* **289,** 1197–1202 (2000).
42. Zhang, L. *et al.* Gene expression profiles in normal and cancer cells. *Science* **276,** 1268–1272 (1997).
43. Wenzel, S. E. Eosinophils in asthma—closing the loop or opening the door? *N. Engl. J. Med.* **360,** 1026–1028 (2009).

Supplementary Information is linked to the online version of the paper at www.nature.com/nature.

Acknowledgements We thank R. King, L. Xu, M. McConnell, K. Emerson, G. R. Pattison and M. Mingler for technical assistance, J. M. Farber for the gift of a reagent, R. J. Kryscio for statistical guidance, and B. Appukuttan, M. W. Fannon, R. Mohan, A. P. Pearson, A. M. Rao, G. S. Rao and K. Ambati for discussions. J.A. was supported by National Eye Institute/National Institutes of Health (NIH) grants EY015422, EY018350 and EY018836, the Doris Duke Distinguished Clinical Scientist Award, the Burroughs Wellcome Fund Clinical Scientist Award in Translational Research, the Macula Vision Research Foundation, the E. Matilda Ziegler Foundation for the Blind, the Dr. E. Vernon Smith and Eloise C. Smith Macular Degeneration Endowed Chair, the Lew R. Wassermann Merit & Physician Scientist Awards (Research to Prevent Blindness, RPB), the American Health Assistance Foundation, and a departmental unrestricted grant from the RPB. J.Z.B. was supported by the University of Kentucky Physician Scientist Award. M.E.K. was supported by the International Retinal Research Foundation Dr. Charles Kelman Postdoctoral Scholar Award. R.J.C.A. was supported by Fight for Sight. B.K.A. was supported by NIH grants EY017182 and EY017950, the VA Merit Award and the Department of Defense. M.E.R. was supported by NIH grants AI45898 and DK076893. C.J.G. was supported by NIH grant AI039759. M.E.H. was supported by NIH grants EY017011 and EY015130 and a RPB departmental unrestricted grant. J.R.S. was supported by NIH grant EY010572, and RPB Career Development Award and a departmental unrestricted grant.

Author Contributions A.T., J.Z.B., M.E.K., W.G.C., M.N., K.Y., H.K., R.J.C.A., S.D., K.S., B.J.R., M.G.G., S.J.B., P.G. and A.M. performed experiments. S.G., A.A.H., Y.P., J.D.W., J.R.S., Y.O. and T.I. provided reagents. J.A. conceived and directed the project, and, with assistance from B.K.A., M.E.H., M.E.R., R.J.C.A. and J.R.S., wrote the paper. All authors had the opportunity to discuss the results and comment on the manuscript.

Author Information Reprints and permissions information is available at www.nature.com/reprints. The authors declare competing financial interests: details accompany the full-text HTML version of the paper at www.nature.com/nature. Correspondence and requests for materials should be addressed to J.A. (jamba2@email.uky.edu).

METHODS

Human tissue. Choroidal neovascular tissue was excised from patients with AMD who had no prior treatment for CNV. Retinal fibrosis tissue was excised from patients with a diagnosis of epiretinal membrane formation. Donor eyes from patients with atrophic AMD without CNV and patients without AMD were obtained from eye banks. Eyes with choroidal melanoma were obtained by surgical enucleation. The study followed the guidelines of the Declaration of Helsinki. Institutional review boards granted approval for allocation and histological analysis of specimens.

Animals. All animal experiments were in accordance with the guidelines of the University of Kentucky Institutional Animal Care and Use Committee and the Association for Research in Vision and Ophthalmology. C57BL/6J and $Kit^{W\text{-}v}$/$Kit^{W\text{-}v}$ mice were purchased from The Jackson Laboratory. $Ccr3^{-/-}$, $Ccl11^{-/-}$, $Ccl24^{-/-}$, $Ccl11^{-/-}$ $Ccl24^{-/-}$ and Δdbl GATA mice have been previously described[11,12,25,26]. $Ccl2^{-/-}$ $Ccr2^{-/-}$ mice were generated by interbreeding single knockout mice described previously[32].

Drug injections. Rat IgG2a neutralizing antibody against mouse CCR3 (R&D Systems), control rat IgG2a (Serotec), goat neutralizing antibody against mouse CCL11 (1 μg; R&D Systems), goat neutralizing antibody against mouse CCL24 (5 μg; R&D Systems), control goat IgG (Jackson Immunoresearch), or (*S*)-methyl-2-naphthoylamino-3-(4-nitrophenyl)propionate (SB328437; Calbiochem) dissolved in DMSO were injected into the vitreous humour of mice using a 33-gauge double-calibre needle (Ito Corporation) once, immediately after laser injury as previously described[22].

Flow cytometry. Rat antibody against mouse CCR3 (1:250; Santa Cruz) coupled with phycoerythrin (PE)-donkey antibody against rat IgG (1:250; Jackson Immunoresearch) or AlexaFluor647-conjugated rat antibody against mouse CCR3 (10 μg ml^{-1}; BD Biosciences) were used to quantify cell surface receptor expression on CECs, defined by CD31$^+$ VEGFR-2$^+$ expression, gated by FITC-conjugated rat antibody against mouse CD31 (20 μg ml^{-1}; BD Biosciences) and PE-conjugated rat antibody against mouse VEGFR-2 (20 μg ml^{-1}; BD Biosciences). Macrophages, neutrophils, eosinophils and mast cells were defined as F4/80$^+$ CD11c$^-$, Gr-1$^+$ F4/80$^-$, CCR3^{hi} CD3$^-$ CD117^{int} CD49d$^+$ and CCR3^{int} CD3$^-$ CD117^{hi} CD49d$^+$ cells, respectively. The DNA content for cell cycle was analysed after incubation with propidium iodide (0.05 mg ml^{-1}; Molecular Probes) containing 0.1% Triton X-100 and RNase A (0.1 mg ml^{-1}; Roche). Samples were analysed on a LSRII (Becton Dickinson).

Immunolabelling. Immunofluorescent staining was performed with antibodies against human CCR3 (rat monoclonal, R&D Systems) or human CD31 (mouse monoclonal, Dako), and identified with Alexa 488 (Molecular Probes) or Cy3 secondary antibodies (Jackson ImmunoResearch). Immunohistochemical staining with the primary antibodies specific for human eotaxins-1, -2 and -3 (mouse monoclonal, R&D Systems) was performed using horseradish peroxidase. Laser-injured mouse eye sections were stained with antibodies against mouse CCL11 or CCL24 (both R&D Systems) along with antibody against mouse CD31 (BD Biosciences) and visualized with FITC or Cy3 secondary antibodies. Images were obtained using Leica SP5 or Zeiss Axio Observer Z1 microscopes.

Tube formation assay. Ninety-six-well plates were coated with Growth-Factor-Reduced Matrigel (BD Biosciences) mixed with rat neutralizing-antibody against human CCR3 (20 μg ml^{-1}, R&D Systems) or control rat IgG2a (Invitrogen) and allowed to solidify in the incubator at 37 °C for 45 min. Human CECs[44–47] were plated on top of the Matrigel at 2.25×10^4 cm^{-2} in EBM-2 basal media (Cambrex) containing 1% FBS with CCR3 antibody or rat IgG2a at the concentrations shown and allowed to grow overnight. Tube formation was analysed by counting the number of cell junctions per mm^2.

Proliferation assay. Human CECs were synchronized for cell cycle state by first cultivating them in EGM2-MV media (Lonza) supplemented with 10% FBS (Gibco) to achieve complete confluence, and then by overnight serum starvation in MCDB131 media (Gibco) with 0.1% FBS. They were passaged to 96-well plates at a density of 5,000 cells per well, followed by stimulation for 24 h with eotaxin-1, 2 or 3 (10 ng, 100 ng and 2 μg per ml, respectively; Peprotech) in MCDB131 media with 0.1% FBS. After 24 h, cell viability was measured with BrdU ELISA (Chemicon) according to the manufacturer's instructions.

F-actin polymerization assay. Human CECs were seeded in black-walled 96-well plates and grown to 70–80% confluence in fully supplemented EGM-2MV. Cultures were serum-starved overnight in basal media and then stimulated with recombinant human eotaxin-1 (10 ng ml^{-1}), eotaxin-2 (100 ng ml^{-1}), eotaxin-3 (2 μg ml^{-1}) (Peprotech), or vehicle control (PBS). At 0, 10, 30, 60 or 120 s time-points, cells were fixed in 3.7% paraformaldehyde for 10 min, washed, permeabilized in PBS with 0.1% Triton X-100, and then stained with rhodamine-labelled phalloidin (1:200, Invitrogen) as per the manufacturer's recommendations. Plates were analysed on a fluorescent plate reader (Synergy 4, Biotek) followed by fluorescent microscopy (Nikon E800).

Migration assay. Eotaxins-1, -2 and -3 were reconstituted in 0.1% BSA and then mixed with Matrigel diluted 1:1 with serum-free endothelial basal media (EBM-2; Lanza). Five-hundred microlitres of EBM-2 was added to each well of a 24-well plate, followed by a 6.5-mm diameter Transwell insert (8 μm pores; Corning). Human CECs in EBM-2 were prestained with Vybrant DiO (Invitrogen) for 30 min at 37 °C and seeded into the inserts at 50,000 cells per 200 μl of serum free EBM-2 media. The plates were allowed to incubate for 16 h at 37 °C, 5% CO_2. The migrated cells were imaged with an Olympus CK40 microscope and Olympus DP71 camera.

RAC1 activation. Human CECs were cultured in EGM-2 MV containing 5% FBS. Before starting the assay, cells were serum-starved overnight using basal medium (MCDB131) supplemented with 1% FBS. Cells were stimulated for designated times with eotaxin-1, -2 and -3 (10 ng ml^{-1}, 100 ng ml^{-1} and 2 μg ml^{-1}, respectively). Equal amounts of lysates (500 μg) were incubated with GST–Pak1–PBD agarose beads (Upstate) to pull down active GTP-bound RAC1 at 4 °C for 1 h with rotation. The samples were subsequently analysed for bound RAC1 by western blot analysis using an anti-RAC1 antibody (Upstate).

Electroretinography. Mice were dark-adapted overnight and then anaesthetized. Both eyes were positioned within a ColourBurst Ganzfeld stimulator (Diagnosys). Espion software (Diagnosys) was used to program a fully automated flash intensity series, from which retinal responses were recorded.

44. Geisen, P., McColm, J. R. & Hartnett, M. E. Choroidal endothelial cells transmigrate across the retinal pigment epithelium but do not proliferate in response to soluble vascular endothelial growth factor. *Exp. Eye Res.* **82**, 608–619 (2006).
45. Peterson, L. J., Wittchen, E. S., Geisen, P., Burridge, K. & Hartnett, M. E. Heterotypic RPE-choroidal endothelial cell contact increases choroidal endothelial cell transmigration via PI 3-kinase and Rac1. *Exp. Eye Res.* **84**, 737–744 (2007).
46. Smith, J. R. *et al.* Unique gene expression profiles of donor-matched human retinal and choroidal vascular endothelial cells. *Invest. Ophthalmol. Vis. Sci.* **48**, 2676–2684 (2007).
47. Zamora, D. O. *et al.* Proteomic profiling of human retinal and choroidal endothelial cells reveals molecular heterogeneity related to tissue of origin. *Mol. Vis.* **13**, 2058–2065 (2007).

Laser Scanning Tomography of Optic Discs of the Normal Japanese Population in a Population-based Setting

Haruki Abe, MD, PhD,[1] Motohiro Shirakashi, MD, PhD,[1] Tae Tsutsumi, MD,[2,3] Makoto Araie, MD, PhD,[3] Atsuo Tomidokoro, MD, PhD,[3] Aiko Iwase, MD, PhD,[2] Goji Tomita, MD, PhD,[4] Tetsuya Yamamoto, MD, PhD,[5] Tajimi Study Group

Objective: To evaluate the optic disc characteristics using the Heidelberg retina tomograph (HRT) II in a large sample of normal Japanese subjects.

Design: Cross-sectional study.

Participants: A total of 3576 eyes of 2036 normal subjects, with good-quality HRT II images, of 6042 eyes of 3021 subjects aged 40 years or more who participated in the Tajimi Study, a population-based eye study in Japan.

Methods: Optic disc parameters were obtained using HRT II, and the association of gender, age, height, weight, blood pressure, ocular perfusion pressure, refraction, intraocular pressure (IOP), central corneal thickness (CCT), and disc size on HRT parameters was assessed using simple and multiple regression analyses.

Main Outcome Measures: HRT parameters, including disc area, cup area, rim area, cup-to-disc area ratio, cup volume, rim volume, mean cup depth, maximum cup depth, height variation contour, cup shape measure, mean retinal nerve fiber layer (RNFL) thickness, and RNFL cross-sectional area, and the crude and partial correlations of the potential confounders with the HRT parameters.

Results: Disc area, cup-to-disc area ratio, and rim area averaged 2.06 ± 0.41 mm^2 (mean$\pm$standard deviation), 0.23 ± 0.13, and 1.55 ± 0.29 mm^2, respectively. All HRT parameters were strongly or moderately correlated between right and left eyes (Pearson's correlation coefficients = 0.45–0.83, $P<0.001$). Absolute inter-eye differences in several HRT parameters were positively correlated with disc area ($P<0.05$). Multiple regression analyses adjusting for the confounders showed weak but significant correlations of height, refractive error, IOP, and CCT with several HRT parameters (partial correlation coefficient (absolute value) = 0.04–0.16, $P<0.05$), and moderate or weak but significant correlations of disc area with all HRT parameters (partial correlation coefficient [absolute value] = 0.05–0.73, $P<0.05$). Gender, weight, blood pressure, and ocular perfusion pressure did not significantly correlate with HRT parameters.

Conclusions: This report presents reference data of normality for the HRT parameters based on a large sample of normal Japanese subjects. There were small but significant influences of height, refractive error, IOP, and CCT on several HRT parameters. Many HRT parameters were moderately or weakly affected by disc size.

Financial Disclosure(s): Proprietary or commercial disclosure may be found after the references.
Ophthalmology 2009;116:223–230 © 2009 by the American Academy of Ophthalmology.

Because structural changes of the optic disc often precede the development of visual field loss in glaucoma,[1–5] detection of optic disc damage plays a vital role in the diagnosis of glaucoma, especially in its early stages. Although ophthalmoscopy and fundus photography are still widely used for assessing glaucomatous optic disc damage, they are limited by their subjective and qualitative nature.[6–8] With the development of optic nerve imaging instruments, objective and quantitative measurements of the optic disc have become available. A confocal scanning laser ophthalmoscope, such as the Heidelberg retina tomograph (HRT) or HRT II (Heidelberg Engineering, Heidelberg, Germany), allows 3-dimensional topographic analysis of the optic disc and provides a quantitative measure of a variety of optic disc parameters.[9–12]

Understanding of normal optic disc shape and related factors are of critical importance in improving the performance of confocal scanning laser ophthalmoscope to determine glaucomatous changes in the optic disc. Distributions or ranges of the optic disc parameters determined with confocal scanning laser ophthalmoscope in large samples of normal subjects (number of subjects $>\sim500$) have been reported by Hermann et al.[13] (1764 eyes of 882 subjects) and Vernon et al.[14] (918 eyes of 459 subjects) in white populations. Because there are racial differences in optic disc characteristics,[15–19] it is worthwhile accumulating such

ISSN 0161-6420/09/$–see front matter
doi:10.1016/j.ophtha.2008.09.013

information for each of the various ethnicities. For Asian populations, however, to our knowledge, there are only the Turkish hospital-based study by Durukan et al.[20] (1102 eyes of 551 subjects) and 2 Japanese hospital-based studies with relatively small sample sizes by Nakamura et al.[21] (77 eyes of 77 subjects) and Uchida et al.[22] (223 eyes of 223 subjects).

We recently conducted the Tajimi Study, a population-based eye study focusing primarily on estimating the prevalence of glaucoma among Japanese persons aged 40 years or more.[23–27] The purposes of the present report were to evaluate the optic disc characteristics by means of HRT II in a large sample of ophthalmologically normal Japanese subjects who participated in the Tajimi Study and to evaluate associations of possibly related systemic and ocular factors, including gender, age, height, weight, blood pressure, ocular perfusion pressure (OPP), refractive error, intraocular pressure (IOP), central corneal thickness (CCT), and optic disc size with the optic disc characteristics.

Subjects and Methods

Population Sampling

The Tajimi Study, a population-based eye study of Japanese subjects aged 40 years or more was conducted between September of 2000 and October of 2001 in Tajimi City, Japan.[23–27] The details of the Tajimi Study have been published.[23–27] Briefly, of 54,165 inhabitants aged 40 years or more in Tajimi City as of August 1, 2000, 4000 were selected randomly without stratification and were encouraged to participate in the epidemiologic study. The investigation followed the tenets of the World Medical Association's Declaration of Helsinki and the municipal statutes of Tajimi City for protecting personal information; the study protocol was approved by the ethics committee of Tajimi City. Written informed consent was obtained from all participants after the details of the study had been explained fully. Among the selected 4000 participants, 48 died and 82 were not actual residents of or had moved from Tajimi City during the screening period. Of the remaining 3870 persons, 3021 participated in the screening examinations.

Ocular Examinations

Screening and definitive examinations have been reported in detail.[23–27] Briefly, the screening examinations included not only ocular parameters but also parameters such as height, weight, and blood pressure. OPP was calculated as "2/3[diastolic blood pressure + 1/3(systolic blood pressure—diastolic blood pressure)]–IOP." The ocular examinations included measurement of refractive status and corneal curvature using an autorefractometer (KP-8100PA, Topcon, Tokyo, Japan), visual acuity using a Landolt ring chart at a distance of 5 m with refractive correction, and CCT using a specular-type pachymeter (SP-2000P, Topcon), slit-lamp biomicroscopic examination, evaluation of angle width according to the van Herick method, IOP measurement by Goldmann applanation tonometry, fundus examination based on digital color photographs obtained through an undilated pupil using the IMAGEnet digital fundus camera system (TRC-NW6S, Topcon) with angles of 30 and 45 degrees, visual field screening using a frequency doubling technology screener (Humphrey Instruments, San Leandro, CA) with the C-20–1 screening test, and optic disc measurements using HRT II (software version 1.4.1). Participants were referred for definitive examination if ocular disorders or related conditions were suspected and if they met 1 or more of the following criteria: corrected visual acuity <20/30; abnormal findings on slit-lamp examination or on fundus photographs; IOP >19 mmHg (i.e., mean + 2 × standard deviation of the IOP values previously reported in ~12,000 Japanese eyes[28]); angle width grade 2 or less (van Herick method); findings in the optic disc, retina, or both suggestive of glaucoma or other ocular diseases; and at least 1 abnormal test point in the frequency doubling technology visual field test. The definitive examination included slit-lamp examination, gonioscopy, optic disc and posterior pole fundus evaluation with a Goldmann 2-mirror lens (Haag-Streit, Koeniz, Switzerland), applanation tonometry, and visual field testing with the Humphrey Perimeter Central 30–2 Swedish Interactive Threshold Algorithm Standard program (Humphrey Instruments). Unless gonioscopy revealed an occludable angle, the pupil was dilated to obtain stereoscopic disc photographs (3-DX NM; Nidek, Gamagori, Japan) and to observe the ocular fundus in detail by indirect ophthalmoscopy. When the angle was thought to be occludable, the same examinations were carried out with undilated pupils.

Optic Disc Measurements using HRT II

In the screening examination, optic disc parameters were measured using HRT II. HRT II uses a diode laser (670-nm wavelength) to sequentially scan the retinal surface in the horizontal and vertical directions at multiple focal planes. By using confocal scanning principles, a 3-dimensional topographic image is constructed from a series of optical image sections at consecutive focal planes. The topographic image determined from the acquired 3-dimensional image consists of 384×384 (147,456) pixels, each of which is a measurement of retinal height at its corresponding location. For every subject in this study, images were obtained through undilated pupils with a 15-degree field of view. Three topographic images were obtained, combined, and automatically aligned to make a single mean topographic image for analysis. A contour line of the optic disc margin was drawn around the inner margin of the peripapillary scleral ring by one experienced examiner (TT), who was masked to the other clinical information, with viewing nonstereo color fundus photographs. The contour line was reviewed in the topography and reflectance images and the height profile graph included in the instrument by the same examiner. For approximately 500 HRT images randomly chosen, another experienced examiner (GT) double-checked the contour lines and confirmed the correctness of the placement. Twelve HRT parameters obtained with routine analysis were analyzed: disc area, cup area, rim area, cup-to-disc area ratio, cup volume, rim volume, mean cup depth, maximum cup depth, height variation contour, cup shape measure, mean retinal nerve fiber layer (RNFL) thick-

ness, and RNFL cross-sectional area. Magnification errors were corrected using subjects' refractive status and corneal curvature measurements. This instrument and these parameters have been described.[14,17,20,29]

Data Analysis

In the present study, the analysis was restricted to eyes that had valid optic disc measurements with HRT II. Good image quality was defined by appropriate focus, brightness and clarity, minimal eye movement, optic disc centered in the image, and a standard deviation of the mean topographic image <40 μm. Eyes in which good-quality images could not be obtained were excluded from the analysis. Eyes of normal subjects based on the screening and definitive examinations were included in the analysis. Normal subjects had a best corrected visual acuity ≥20/30, spherical refraction ≤±5 diopters (D), cylinder correction ≤±3 D, a normal IOP ≤21 mmHg, normal appearance of the optic disc and ocular fundus, normal visual field by frequency doubling technology screener or Humphrey perimeter, no previous laser surgery or intraocular surgery, and no significant ocular disease. Patients with glaucoma, suspected glaucoma, IOP >21 mmHg, or exfoliation in at least 1 eye or those with eyes having any inborn aberrations (e.g., tilted disc) were carefully excluded.

Data were analyzed using SPSS 14.0J for Windows (SPSS Japan, Inc., Tokyo, Japan). Comparisons between groups were analyzed with paired or unpaired *t* test or the chi-square test. Pearson's correlation coefficients were calculated to assess correlations between the 2 variables. Multiple regression analysis was applied to adjust for the effects of potential confounders. All tests were 2-tailed. Because the sample size in the current report was sufficiently large (i.e., >1700 right and 1800 left eyes), parametric tests, including *t* test, Pearson's correlation coefficient, and multiple regression, were used based on the central limit theorem.

Results

Of 6042 eyes of the 3021 participants of the Tajimi Study, reliable HRT II results in ophthalmologically normal eyes were analyzed in 3576 eyes (1769 right eyes and 1807 left eyes) of 2036 participants. Between the included and excluded subjects, the male/female ratio was not statistically different (924/1112 vs. 410/575, $P = 0.051$, χ^2 test), whereas age was significantly younger in the included subjects than in the excluded subjects (56.0±10.0 years vs. 63.4±13.7 years, $P<0.001$, unpaired *t* test). The reasons for exclusion were (1) subjects were screened in their own home (88 eyes); (2) HRT II measurements could not be completed at the screening sites for various reasons, such as subjects' ocular or physical problems (906 eyes); and (3) standard deviation of the HRT II measurements was ≥40 μm (640 eyes). Eyes of definitive glaucoma, suspected glaucoma, pseudoexfoliation, primary angle closure, ocular hypertension or fellow eyes of these eyes (364 eyes), eyes with other ocular diseases including congenital disc anomalies that could affect the disc shape (84 eyes), pseudophakic eyes (41 eyes), eyes with excessive refractive errors (spherical error >±5 D or cylindrical error >±3 D) (260 eyes), and eyes with best corrected visual acuity worse than 20/30 (83 eyes) were also excluded.

Inter-eye Difference in HRT Parameters

HRT parameters were compared between right and left eyes in 1540 normal subjects, of whom both eyes were eligible. All HRT parameters were significantly correlated between right and left eyes (Pearson's correlation coefficients ≥0.450, $P<0.001$) (Table 1 [available at http://aaojournal.org]). Rim volume and height variation contour showed small but significant inter-eye difference ($P<0.001$, paired *t* test), whereas the other parameters did not. The absolute differences in HRT parameters between right and left eyes are also shown in Table 1 (available at http://aaojournal.org). Among HRT parameters, inter-eye absolute difference was significantly different between male and female subjects only in cup shape measure (0.05±0.04 and 0.06±0.05, respectively, $P = 0.001$), and the difference was still significant ($P = 0.027$) in multiple regression analyses adjusting for age, height, weight, systolic and diastolic blood pressure, OPP, refractive error, IOP, and CCT. Multiple regression analyses adjusting for these confounders and gender showed that disc area (mean value of right and left eyes) was significantly positively correlated with inter-eye absolute difference in cup area, rim area, cup volume, rim volume, and RNFL cross-sectional area ($P<0.05$), suggesting subjects having larger discs tended to show greater inter-eye absolute differences in these HRT parameters, whereas disc area was significantly negatively correlated with the inter-eye absolute difference in cup shape measure ($P<0.001$). Because all HRT parameters were significantly correlated and the results of the analyses were similar between right and left eyes, only the results from the right 1769 eyes (787 male and 982 female subjects) are presented in the following sections.

Association of Gender, Age, Height, Weight, and Blood Pressure with HRT Parameters

A total of 787 male subjects had significantly older age, heavier weight, taller height, higher systolic and diastolic blood pressure, and higher OPP and thicker CCT than 982 female subjects (unpaired *t* test, $P\leq0.009$), whereas refractive error and IOP were not significantly different ($P\geq0.126$) (Table 2).

In simple regression analyses, age was negatively correlated with disc area, rim area, rim volume, maximum cup depth, height variation contour, mean RNFL thickness, and RNFL cross-sectional area in both male and female subjects ($P\leq0.002$) (Table 3 [available at http://aaojournal.org]). These trends are also seen after adjusting for the potential confounders using multiple regression analysis (Tables 4 and 5 [available at http://aaojournal.org]). Cup area and cup-to-disc area ratio were significantly greater in male subjects than female subjects ($P\leq0.004$). However, after adjusting for the potential confounders, gender-related dif-

Table 2. Comparison of Demographic Data and Heidelberg Retina Tomograph Parameters of Normal Right Eyes between 787 Male and 982 Female Subjects

	All	Male	Female	P*
Age (y)	55.7±9.8 (55.3–56.2)	56.4±9.8 (55.7–57.1)	55.2±9.9 (54.5–55.8)	0.009
Weight (kg)	58.2±10.6 (57.7–58.7)	63.9±10.1 (63.2–64.6)	53.7±8.9 (53.1–54.3)	<0.001
Height (cm)	158.9±8.8 (158.5–159.3)	165.6±6.7 (165.7–166.1)	153.3±6.3 (152.9–153.8)	<0.001
Systolic blood pressure (mmHg)	130.4±22.7 (129.3–131.4)	133.5±22.3 (131.9–135.1)	128.9±22.8 (127.3–130.5)	<0.001
Diastolic blood pressure (mmHg)	78.8±13.2 (78.1–79.4)	80.9±13.2 (80.0–81.8)	77.2±13.1 (76.3–78.2)	<0.001
OPP (mmHg)	49.5±9.8 (49.1–50.0)	51.1±9.6 (50.4–51.7)	48.5±9.8 (47.8,49.2)	<0.001
Refractive error (diopters)†	−0.4±1.7 (−0.5 to −0.4)	−0.5±1.8 (−0.6 to −0.3)	−0.4±1.8 (−0.6 to −0.3)	0.612
IOP (mmHg)	14.4±2.5 (14.3–14.6)	14.6±2.6 (14.4–14.8)	14.5±2.4 (14.3–14.6)	0.126
CCT (μm)	520±32 (518–521)	525±33 (523–527)	516±31 (514–518)	<0.001
Disc area (mm^2)‡	2.06±0.41 (2.04–2.08)	2.08±0.44 (2.04–2.11)	2.05±0.39 (2.02–2.08)	0.085
Cup area (mm^2)‡	0.51±0.35 (0.49–0.53)	0.54±0.37 (0.51–0.56)	0.50±0.32 (0.47–0.52)	0.002
Rim area (mm^2)‡	1.55±0.29 (1.54–1.56)	1.54±0.29 (1.52–1.56)	1.55±0.29 (1.53–1.57)	0.181
Cup-to-disc area ratio‡	0.23±0.13 (0.23–0.24)	0.24±0.13 (0.23–0.25)	0.23±0.12 (0.22–0.24)	0.004
Cup volume (mm^3)‡	0.11±0.12 (0.11–0.12)	0.12±0.12 (0.11–0.13)	0.11±0.11 (0.10–0.12)	0.006
Rim volume (mm^3)‡	0.41±0.14 (0.40–0.42)	0.40±0.14 (0.39–0.41)	0.42±0.14 (0.41–0.43)	0.083
Mean cup depth (mm)‡	0.21±0.09 (0.20–0.21)	0.21±0.09 (0.20–0.22)	0.20±0.09 (0.20–0.21)	0.034
Maximum cup depth (mm)‡	0.57±0.20 (0.56–0.58)	0.58±0.20 (0.56–0.59)	0.57±0.21 (0.56–0.59)	0.157
Height variation contour (mm)‡	0.38±0.09 (0.38–0.39)	0.38±0.10 (0.38–0.39)	0.39±0.10 (0.38–0.39)	0.572
Cup shape measure‡	−0.19±0.07 (−0.19 to −0.19)	−0.19±0.07 (−0.19 to −0.18)	−0.19±0.07 (−0.20 to −0.19)	0.033
Mean RNFL thickness (mm)‡	0.25±0.07 (0.25–0.26)	0.25±0.07 (0.25–0.25)	0.26±0.07 (0.25–0.26)	0.007
RNFL cross-sectional area (mm^2)‡	1.29±0.35 (1.27–1.30)	1.27±0.35 (1.24–1.29)	1.31±0.35 (1.28–1.33)	0.028

RNFL = retinal nerve fiber layer; OPP = ocular perfusion pressure; IOP = intraocular pressure; CCT = central corneal thickness.
Data are shown as "mean±standard deviation (95% confidence interval)."
*P value on comparison between male and female subjects (unpaired t test).
†Spherical equivalent values.
‡Because of multiple comparisons among the 12 Heidelberg Retina Tomograph parameters, Bonferroni correction was applied with a level of significance of 0.0042.

ference in HRT parameters did not reach statistical significance ($P>0.05$) (Tables 4 and 5 [available at http://aaojournal.org]). Height was also weakly correlated with several HRT parameters in simple and multiple regression analyses (Tables 3, 4, and 5 [available at http://aaojournal.org]). Although disc area was not significantly correlated with height in multiple regression analysis, cup-related parameters were positively correlated with height, whereas rim-related parameters were negatively correlated with height (Tables 4 and 5 [available at http://aaojournal.org]). Weight was not correlated significantly with any HRT parameters in multiple regression analyses (Tables 4 and 5 [available at http://aaojournal.org]). Systolic blood pressure and OPP were negatively correlated with some HRT parameters in simple regression analyses, but the significant correlations disappeared after adjusting for the potential confounders (Tables 3, 4, and 5 [available at http://aaojournal.org]).

Association of Refractive Error, IOP, and CCT with HRT Parameters

Multiple regression analysis showed weak but significant positive correlation between refractive error and disc area ($P<0.001$), suggesting the trend that more myopic eyes had smaller discs (Table 4 [available at http://aaojournal.org]). Rim volume, mean RNFL thickness, and RNFL cross-sectional area were negatively correlated with refractive error in both male and female subjects in simple regression analyses ($P<0.001$) and multiple regression analyses ($P<0.001$) (Tables 3 and 4 [available at http://aaojournal.org]), suggesting that more myopic eyes had greater rim volume. Rim volume, mean RNFL thickness, and RNFL cross-sectional area were still negatively correlated with refractive error after adjusting for disc area and the other potential confounders (Table 5 [available at http://aaojournal.org]).

IOP was positively correlated with some cup-related parameters in multiple regression analyses ($P<0.05$) (Table 5 [available at http://aaojournal.org]), suggesting the trend that eyes with higher IOP had greater cup. CCT showed weak but significant negative correlations with cup volume in multiple regression analyses ($P<0.05$) (Tables 4 and 5 [available at http://aaojournal.org]).

Association of Disc Area with the Other HRT Parameters

Disc area was correlated with all HRT parameters except height variation contour with P values of ≤ 0.001 (Table 6 [available at http://aaojournal.org]). Cup area and cup volume were relatively strongly correlated with disc area (Pearson's correlation coefficients ≥ 0.61). In multiple regression analyses after adjusting for the potential confounders, disc area was also correlated with all HRT parameters except height variation contour with P values <0.001 (Table 5).

Discussion

A total of 3576 eyes of 2036 ophthalmologically normal Japanese subjects who participated in the Tajimi Study[23–27] were included in the present analyses. The age distribution of the Tajimi Study participants was similar to that of the Japanese population.[23,30] In the Tajimi Study, although the distribution of IOP was widely overlapped between normal and glaucoma eyes,[23] the criteria for diagnosing glaucoma were not based on IOP, but on findings in the visual field and optic disc in accordance with the criteria of the International Society for Geographical and Epidemiological Ophthalmology.[31] Moreover, ophthalmologically normal eyes in the current analyses were selected according to more strict criteria as described previously. Thus, these criteria should achieve reasonably high specificity of normal eyes in the present report.

In the present report, descriptive statistics of the HRT parameters in the population were presented. All HRT parameters were strongly or moderately correlated between right and left eyes. Absolute inter-eye differences in several HRT parameters were positively correlated with disc area. Multiple regression analyses adjusting for the potential confounders showed weak but significant correlations of height, refractive error, IOP, and CCT with several HRT parameters, and moderate or weak but significant correlations of disc area with many HRT parameters. Gender, weight, blood pressure, and OPP did not significantly correlate with HRT parameters.

Several investigators have reported racial differences in optic disc characteristics.[15–19] In normal subjects of various races, Tsai et al.,[15] using HRT, found that disc area, cup area, cup-to-disc area ratio, cup volume, and maximum cup depth were significantly greater in 43 African-Americans than in 44 whites, with intermediate values for 45 Asians and 48 Hispanics. In another study of normal subjects, Girkin et al.,[17] using HRT II, found significantly greater disc area, cup area, rim area, cup volume, mean cup depth, and mean RNFL thickness in 144 normal eyes (84 subjects) of African-Americans than in 109 normal eyes of 68 white subjects. In normal white subjects, Hermann et al.,[13] using HRT, reported that the mean disc area was 1.82 mm^2 (882 subjects), and Vernon et al.[14] (459 subjects), using HRT II, reported that the mean and median disc areas were 1.98 and 1.93 mm^2, respectively. Girkin et al.,[17] using HRT II, reported that the mean disc areas were 2.26 mm^2 for normal African-American subjects and 1.98 mm^2 for normal white subjects. In the present report on 2036 normal Japanese subjects using HRT II, the mean disc area was 2.06 mm^2 (Table 2). The normal range of disc area was between 1.36 and 3.00 mm^2 in the current population if the normal range is defined between the 2.5 and 97.5 percentiles. The mean value of the disc area in the present report tended to be greater than that in normal white subjects[13,14] but smaller than that in normal black subjects.[17]

The characteristics of optic discs are usually well correlated between right and left eyes in each subject. One of the established criteria for diagnosing glaucoma in population-based studies, such as "difference of the vertical cup-to-disc ratio is 0.2 or more between both eyes,"[23,31–34] is based on the inter-eye similarity in optic disc shape in normal eyes. In previous studies, one study of 551 normal Turkish subjects found no significant inter-eye differences in HRT parameters,[20] whereas other studies on normal white subjects reported significant inter-eye differences in some HRT parameters, although the differences were small.[13,35,36] In the present report, all HRT parameters were strongly or moderately correlated between right and left eyes and no apparently significant inter-eye difference was found as a whole in all parameters except rim volume and height variation contour (Table 1 [available at http://aaojournal.org]). However, the absolute inter-eye differences in some parameters were not as small as clinically ignorable. For example, absolute inter-eye difference in cup-to-disc area ratio (0.07) was equivalent to 30% of the bilateral mean (0.23) of the parameter. Thus, the current results indicate that inter-eye difference in HRT parameters is not always small enough in each individual and that it cannot be adopted as a useful diagnostic tool in detecting disc pathology, especially among subjects with large optic discs because the absolute inter-eye difference was positively correlated with the optic disc size.

Several studies have reported significant gender-related differences in HRT parameters.[13–15,20,22] In normal subjects of various races, Tsai et al.,[15] using analysis of variance, found that women had a significantly greater rim volume and that men had significantly greater cup area, cup-to-disc area ratio, cup volume, and cup-to-disc ratio. In normal Turkish subjects, Durukan et al.,[20] using the *t* test, found that women had significantly greater height variation contour, mean RNFL thickness, and RNFL cross-sectional area. In normal white subjects, Hermann et al.[13] and Vernon et al.,[14] using the Mann-Whitney test, found that the women had significantly greater rim volume, mean RNFL thickness, and RNFL cross-sectional area. In Japan, Uchida et al.,[22] using the Mann-Whitney test, found that men had significantly greater disc area. However, none of these investigators adjusted for other important potential confounders such as age, height, and refraction using multiple regression analysis. In the present report, some HRT parameters were significantly different between male and female subjects using unpaired *t* test (Table 2), but the significant differences diminished after adjusting for the potential confounders using multiple regression analysis (Tables 4 and 5 [available at http://aaojournal.org]). Thus, gender itself is not thought to influence HRT parameters.

Between age and optic disc characteristics, several investigators observed significant association,[20–22,37–39] whereas others did not.[13,14,16,40,41] In normal white subjects, Hermann et al.,[13] using HRT, reported that although the disc area and mean RNFL thickness were smaller in older subjects (age, 52–70 years) than in younger subjects (35–40 years), no significant differences were noted. Vernon et al.[14] found no significant age-related differences in HRT parameters in normal white subjects, although rim and RNFL-related parameters tended to decrease with age. In contrast, although they were hospital-based studies and the numbers of subjects were not sufficiently large, one study of normal Japanese subjects found that mean RNFL thickness and RNFL cross-sectional area significantly decreased with in-

creasing age,[21] and another study found that rim volume, height variation contour, mean RNFL thickness, and RNFL cross-sectional area significantly decreased with increasing age and that cup shape measure significantly increased with increasing age.[22] In the present report, several HRT parameters, including disc area, correlated with age in both crude and partial correlation analyses. Approximately one third of the study participants had to be excluded from the analysis of HRT data, and because there was significant difference in age between the included and excluded subjects, the association of age with HRT parameters in the included subjects should be interpreted with caution. For example, the association between older age and smaller disc area may be attributable to the cohort effect than to the longitudinal effect because disc size is supposed to be unchanged throughout lifetime. However, this significant correlation between age and some HRT parameters indicates the importance of adjusting for age as a possible confounder in multiple regression analyses in the current subjects. After adjusting for disc area and the other potential confounders, rim area, rim volume, height variation contour, mean RNFL thickness, and RNFL cross-sectional area significantly decreased with increasing age, whereas cup area, cup-to-disc area ratio, and cup shape measure significantly increased with increasing age (Table 5 [available at http://aaojournal.org]). Our findings are consistent with those of the above previous studies of normal Japanese subjects. If age-related decrease in nerve fibers exists,[42–45] it is possible that HRT parameters that reflect the amount of nerve fibers may slightly decrease with increasing age.

In the present report, partial correlation analyses showed that disc area was not correlated with height, whereas some of the other HRT parameters were significantly correlated with height (Tables 4 and 5 [available at http://aaojournal.org]). After adjusting for the potential confounders, with increasing height, cup-related parameters weakly but significantly increased, whereas rim-related parameters weakly but significantly decreased. In contrast with our findings, the investigators of the Rotterdam Study, using image analysis of stereoscopic optic disc photographs, found no significant height-related differences in cup area and cup-to-disc area ratio.[41] Although the reasons for the discrepancy are unclear, racial differences and differences in methods of evaluating optic disc morphology are at least partially responsible.

In the present report of normal subjects (spherical refraction $\leq \pm 5$D and cylinder correction $\leq \pm 3$ D), both crude and partial correlation analyses showed that several HRT parameters weakly correlated with refractive error (Tables 3, 4, and 5 [available at http://aaojournal.org]). After adjusting for the potential confounders, disc area significantly decreased with an increase in myopia (Table 4 [available at http://aaojournal.org]). After adjusting for disc area and the other potential confounders, rim volume, height variation contour, mean RNFL thickness, and RNFL cross-sectional area significantly increased with an increase in myopia (Table 5 [available at http://aaojournal.org]). Some studies showed a significant influence of refractive errors on HRT parameters.[15,21] Tsai et al.[15] found that rim volume significantly increased with an increase in myopia in normal subjects of various races (refractive error between −6 and +3 D). Nakamura et al.[21] found that mean cup depth and maximum cup depth significantly increased with an increase in myopia in a relatively small sample of normal Japanese subjects (77 subjects, refractive error between −5 and +4.13 D). In contrast, Bowd et al.[38] and Durukan et al.[20] found no significant association between refractive error and HRT parameters in normal white subjects (refractive error $\leq \pm 5$ D) and normal Turkish subjects (refractive error between −4.75 and +4.25 D), respectively. Although the reasons for the differences among these studies and our study, are unclear, differences in sample sizes, subject characteristics, including age, refractive errors, and races, or methods of analyses might have affected the results.

Many studies have reported a significant effect of optic disc size on optic disc characteristics.[13–16,20–22,37,38,40,41] However, in normal Turkish subjects, Durukan et al.[20] found cup shape measure and height variation contour to be independent of disc area. In normal white subjects, Vernon et al.[14] found height variation contour to be the only parameter independent of disc area. Two previous studies of normal Japanese subjects using HRT also found height variation contour to be independent of disc area.[21,22] In the present report, all HRT parameters except height variation contour moderately or weakly correlated with disc area with P values of ≤ 0.001 in both crude and partial correlation analyses (Tables 5 and 6 [available at http://aaojournal.org]). Our findings are consistent with those of previous studies in that height variation contour, which is the height difference between the most elevated and most depressed points of the contour line, is independent of or minimally affected by optic disc size.[14,20–22] On the other hand, as in previous studies,[13–15,20–22,37,38,40] many cup, rim, or RNFL-related HRT parameters were closely influenced by optic disc size, suggesting that optic disc size should be considered in evaluating these parameters.

A recent study reported a significant association between systemic blood pressure and some of the HRT parameters in 232 Greek patients without glaucoma.[46] Topouzis et al[46] found a significant association of lower diastolic blood pressure with increased cup area and decreased rim area in multiple regression analysis. However, Jonas and Gründler[47] analyzed stereo optic disc photographs of 167 normal white subjects and found no significant influence of systemic hypertension on optic disc structure, including disc area and rim area. The present report on normal Japanese subjects did not find a significant association of systemic blood pressure with HRT parameters after adjusting for the possible confounders (Tables 4 and 5 [available at http://aaojournal.org]). Although the true reasons for these discrepancies are hard to be determined, differences in races and blood pressure itself between the studies may be possible explanations.

In the present report, weak but significant correlations between higher IOP and greater cup-related parameters were found in multiple regression analyses including disc area as an independent variable (Table 5). A similar relationship was found in the Blue Mountains Eye Study using optic disc photographs.[48] Investigators of the Beijing Eye Study also reported that rim area evaluated with optic disc photographs was significantly smaller in eyes with IOP >21 mmHg than those with IOP ≤21 mmHg, although, for the

eyes with elevated IOP, neither the optic disc appearance nor the perimetric results were taken into account.[49] These findings, including ours using HRT II, suggest that eyes with higher IOP tend to have greater cup even in normal eyes.

In the present report, after adjusting for the potential confounders, CCT showed weak but significant negative correlations with a few cup-related parameters, suggesting that eyes with a thinner cornea tended to have a greater cup (Tables 4 and 5 [available at http://aaojournal.org]). This may have some clinical implication, if one considers the recently reported findings that thinner cornea is a risk factor for developing glaucoma from ocular hypertensive eyes in the Ocular Hypertension Treatment Study[50] and the European Glaucoma Prevention Study.[51]

One limitation of the present report is the exclusion of a significant proportion of eyes that did not undergo HRT II measurements or in which HRT II images could not be obtained, or those without good-quality optic disc images. Because the excluded subjects were significantly older than the included subjects and age was significantly related to many HRT parameters, the exclusion may have influenced the current results, and the interpretation of age-related changes in HRT parameters in the current subjects should be done with caution. Another limitation of the present report is that only normal subjects with good central vision, no high refractive error, and clear ocular media were included in the analyses. Our definitions of normality may have excluded some potentially normal subjects from the analyses. Despite these limitations, our data provide a reference range of normality for HRT parameters based on a large sample of normal Japanese subjects. The reference range for normality provided in this report becomes a basis for comparison of optic disc characteristics between normal and glaucomatous eyes. Whether the reference range can improve the ability of glaucoma diagnosis in Japanese subjects requires further research.

References

1. Read RM, Spaeth GL. The practical clinical appraisal of the optic disc in glaucoma: the natural history of cup progression and some specific disc-field correlations. Trans Am Acad Ophthalmol Otolaryngol 1974;78:OP255–74.
2. Pederson JE, Anderson DR. The mode of progressive disc cupping in ocular hypertension and glaucoma. Arch Ophthalmol 1980;98:490–5.
3. Zeyen TG, Caprioli J. Progression of disc and field damage in early glaucoma. Arch Ophthalmol 1993;111:62–5.
4. Chauhan BC, McCormick TA, Nicolela MT, LeBlanc RP. Optic disc and visual field changes in a prospective longitudinal study of patients with glaucoma: comparison of scanning laser tomography with conventional perimetry and optic disc photography. Arch Ophthalmol 2001;119:1492–9.
5. Zangwill LM, Weinreb RN, Beiser JA, et al., Confocal Scanning Laser Ophthalmoscopy Ancillary Study to the Ocular Hypertension Treatment Study Group. Baseline topographic optic disc measurements are associated with the development of primary open-angle glaucoma: the Confocal Scanning Laser Ophthalmoscopy Ancillary Study to the Ocular Hypertension Treatment Study. Arch Ophthalmol 2005;123:1188–97.
6. Lichter PR. Variability of expert observers in evaluating the optic disc. Trans Am Ophthalmol Soc 1976;74:532–72.
7. Varma R, Steinmann WC, Scott IU. Expert agreement in evaluating optic discs. Ophthalmology 1992;99:215–21.
8. Azuara-Blanco A, Katz LJ, Spaeth GL, et al. Clinical agreement among glaucoma experts in the detection of glaucomatous changes of the optic disk using simultaneous stereoscopic photographs. Am J Ophthalmol 2003;136:945–50.
9. Mikelberg FS, Wijsman K, Schulzer M. Reproducibility of topographic parameters obtained with the Heidelberg retina tomograph. J Glaucoma 1993;2:101–3.
10. Lusky M, Bosem ME, Weinreb RN. Reproducibility of optic nerve head topography measurements in eyes with undilated pupils. J Glaucoma 1993;2:104–9.
11. Rohrschneider K, Burk RO, Kruse FE, Volcker HE. Reproducibility of the optic nerve head topography with a new laser tomographic scanning device. Ophthalmology 1994;101:1044–9.
12. Ford BA, Artes PH, McCormick TA, et al. Comparison of data analysis tools for detection of glaucoma with the Heidelberg retina tomograph. Ophthalmology 2003;110:1145–50.
13. Hermann MM, Theofylaktopoulos I, Bangard N, et al. Optic nerve morphometry in healthy adults using confocal laser scanning tomography. Br J Ophthalmol 2004;88:761–5.
14. Vernon SA, Hawker MJ, Ainsworth G, et al. Laser scanning tomography of the optic nerve head in a normal elderly population: the Bridlington Eye Assessment Project. Invest Ophthalmol Vis Sci 2005;46:2823–8.
15. Tsai CS, Zangwill L, Gonzalez C, et al. Ethnic differences in optic nerve head topography. J Glaucoma 1995;4:248–57.
16. Varma R, Tielsch JM, Quigley HA, et al. Race-, age-, gender-, and refractive error-related differences in the normal optic disc. Arch Ophthalmol 1994;112:1068–76.
17. Girkin CA, McGwin G Jr, McNeal SF, DeLeon-Ortega J. Racial differences in the association between optic disc topography and early glaucoma. Invest Ophthalmol Vis Sci 2003;44:3382–7.
18. Chi T, Ritch R, Stickler D, et al. Racial differences in optic nerve head parameters. Arch Ophthalmol 1989;107:836–9.
19. Zangwill LM, Weinreb RN, Berry CC, et al., Confocal Scanning Laser Ophthalmoscopy Ancillary Study to the Ocular Hypertension Treatment Study. Racial differences in optic disc topography: baseline results from the Confocal Scanning Laser Ophthalmoscopy Ancillary Study to the Ocular Hypertension Treatment Study. Arch Ophthalmol 2004;122:22–8.
20. Durukan AH, Yucel I, Akar Y, Bayraktar MZ. Assessment of optic nerve head topographic parameters with a confocal scanning laser ophthalmoscope. Clin Experiment Ophthalmol 2004;32:259–64.
21. Nakamura H, Maeda T, Suzuki Y, Inoue Y. Scanning laser tomography to evaluate optic discs of normal eyes. Jpn J Ophthalmol 1999;43:410–4.
22. Uchida H, Yamamoto T, Araie M, et al. Topographic characteristics of the optic nerve head measured with scanning laser tomography in normal Japanese subjects. Jpn J Ophthalmol 2005;49:469–76.
23. Iwase A, Suzuki Y, Araie M, et al., Tajimi Study Group, Japan Glaucoma Society. The prevalence of primary open-angle glaucoma in Japanese: the Tajimi Study. Ophthalmology 2004;111:1641–8.
24. Yamamoto T, Iwase A, Araie M, et al., Tajimi Study Group, Japan Glaucoma Society. The Tajimi Study report 2: prevalence of primary angle closure and secondary glaucoma in a Japanese population. Ophthalmology 2005;112:1661–9.
25. Iwase A, Araie M, Tomidokoro A, et al., Tajimi Study Group. Prevalence and causes of low vision and blindness in a Japa-

nese adult population: the Tajimi Study. Ophthalmology 2006;113:1354–62.
26. Suzuki Y, Iwase I, Araie M, et al., Tajimi Study Group. Risk factors for open-angle glaucoma in a Japanese population: the Tajimi Study. Ophthalmology 2006;113:1613–7.
27. Iwase I, Tomidokoro A, Araie M, et al., Tajimi Study Group. Performance of frequency-doubling technology perimetry in a population-based prevalence survey of glaucoma: the Tajimi Study. Ophthalmology 2007;114:27–32.
28. Shiose Y, Kitazawa Y, Tsukahara S, et al. Epidemiology of glaucoma in Japan—a nationwide glaucoma survey. Jpn J Ophthalmol 1991;35:133–55.
29. Medeiros FA, Zangwill LM, Bowd C, Weinreb RN. Comparison of the GDx VCC scanning laser polarimeter, HRT II confocal scanning laser ophthalmoscope, and Stratus OCT optical coherence tomography for detection of glaucoma. Arch Ophthalmol 2004;122:827–37.
30. Japan 2004/2005 Census [in Japanese]. 62nd ed. Tokyo: Yano Memorial Association Hutoshi Hisashi; 2004:45–52.
31. Foster PJ, Buhrmann R, Quigley HA, Johnson GJ. The definition and classification of glaucoma in prevalence surveys. Br J Ophthalmol 2002;86:238–42.
32. Wolfs RCW, Borger PH, Ramrattan RS, et al. Changing views on open-angle glaucoma: definitions and prevalences—The Rotterdam Study. Invest Ophthalmol Vis Sci 2000;41:3309–21.
33. Quigley HA, West SK, Rodriguez J, et al. The prevalence of glaucoma in a population-based study of Hispanic subjects: Proyecto VER. Arch Ophthalmol 2001;119:1819–26.
34. Rotchford AP, Johnson GJ. Glaucoma in Zulus: a population-based cross-sectional survey in a rural district in South Africa. Arch Ophthalmol 2002;120:471–8.
35. Gherghel D, Orgül S, Prünte C, et al. Interocular differences in optic disc topographic parameters in normal subjects. Curr Eye Res 2000;20:276–82.
36. Hawker MJ, Vernon SA, Ainsworth G, et al. Asymmetry in optic disc morphometry as measured by Heidelberg retina tomography in a normal elderly population: the Bridlington Eye Assessment Project. Invest Ophthalmol Vis Sci 2005;46:4153–8.
37. Garway-Heath DF, Wollstein G, Hitchings RA. Aging changes of the optic nerve head in relation to open angle glaucoma. Br J Ophthalmol 1997;81:840–5.
38. Bowd C, Zangwill LM, Blumenthal EZ, et al. Imaging of the optic disc and retinal nerve fiber layer: the effects of age, optic disc area, refractive error, and gender. J Opt Soc Am A Opt Image Sci Vis 2002;19:197–207.
39. Tsai CS, Ritch R, Shin DH, et al. Age-related decline of disc rim area in visually normal subjects. Ophthalmology 1992;99:29–35.
40. Saruhan A, Orgül S, Koçak I, et al. Descriptive information of topographic parameters computed at the optic nerve head with the Heidelberg retina tomograph. J Glaucoma 1998;7:420–9.
41. Ramrattan RS, Wolfs RC, Jonas JB, et al. Determinants of optic disc characteristics in a general population: the Rotterdam Study. Ophthalmology 1999;106:1588–96.
42. Balazsi AG, Rootman J, Drance SM, et al. The effect of age on the nerve fiber population of the human optic nerve. Am J Ophthalmol 1984;97:760–6.
43. Mikelberg FS, Drance SM, Schulzer M, et al. The normal human optic nerve: axon count and axon diameter distribution. Ophthalmology 1989;96:1325–8.
44. Mikelberg FS, Yidegiligne HM, White VA, Schulzer M. Relation between optic nerve axon number and axon diameter to scleral canal area. Ophthalmology 1991;98:60–3.
45. Jonas JB, Schmidt AM, Muller-Bergh JA, et al. Human optic nerve fiber count and optic disc size. Invest Ophthalmol Vis Sci 1992;33:2012–8.
46. Topouzis F, Coleman AL, Harris A, et al. Association of blood pressure status with the optic disk structure in non-glaucoma subjects: the Thessaloniki Eye Study. Am J Ophthalmol 2006;142:60–7.
47. Jonas JB, Gründler A. Effect of arterial hypertension on the optic disc structure [letter]. Arch Ophthalmol 1996;114:1300–1.
48. Healey PR, Mitchell P, Smith W, Wang JJ. The influence of age and intraocular pressure on the optic cup in a normal population. J Glaucoma 1997;6:274–8.
49. Xu L, Wang Y, Yang H, et al. Size of the neuroretinal rim and optic cup and their correlations with ocular and general parameters in adult Chinese: the Beijing Eye Study. Br J Ophthalmol 2007;91:1616–9.
50. Gordon MO, Beiser JA, Brandt JD, et al., Ocular Hypertension Treatment Study Group. The Ocular Hypertension Treatment Study: baseline factors that predict the onset of primary open-angle glaucoma. Arch Ophthalmol 2002;120:714–20.
51. European Glaucoma Prevention Study (EGPS) Group. Predictive factors for open-angle glaucoma among patients with ocular hypertension in the European Glaucoma Prevention Study. Ophthalmology 2007;114:3–9.

Footnotes and Financial Disclosures

Originally received: March 27, 2008.
Final revision: August 30, 2008.
Accepted: September 7, 2008.
Available online: December 12, 2008. Manuscript no. 2008-400.

[1] Division of Ophthalmology and Visual Sciences, Niigata University Graduate School of Medical and Dental Sciences, Niigata, Japan.

[2] Department of Ophthalmology, Tajimi Municipal Hospital, Tajimi, Japan.

[3] Department of Ophthalmology, University of Tokyo Graduate School of Medicine, Tokyo, Japan.

[4] The Second Department of Ophthalmology, Toho University School of Medicine, Tokyo, Japan.

[5] Department of Ophthalmology, Gifu University Graduate School of Medicine, Gifu, Japan.

Presented in part as a poster at: American Academy of Ophthalmology annual meeting, New Orleans, Louisiana, November 12-13, 2007.

Financial Disclosure(s):
The authors have no proprietary or commercial interest in any materials discussed in this article.

Supported by the Japan National Society for the Prevention of Blindness, Tokyo, Japan, and Japan Ophthalmologists Association, Tokyo, Japan.

Correspondence:
Haruki Abe, MD, PhD, Division of Ophthalmology and Visual Sciences, Niigata University Graduate School of Medical and Dental Sciences, 1-757 Asahimachi-dori, Chuo-ku, Niigata 951-8510, Japan.

Nine-Year Incidence and Risk Factors for Age-Related Macular Degeneration in a Defined Japanese Population

The Hisayama Study

Miho Yasuda, MD, PhD,[1] Yutaka Kiyohara, MD, PhD,[2] Yasuaki Hata, MD, PhD,[1] Satoshi Arakawa, MD,[1] Koji Yonemoto, PhD,[2] Yasufumi Doi, MD, PhD,[3] Mitsuo Iida, MD, PhD,[3] Tatsuro Ishibashi, MD, PhD[1]

Purpose: To estimate the 9-year incidence and risk factors for age-related macular degeneration (AMD) in a general Japanese population.

Design: Population-based, cohort study.

Participants: In 1998, a total of 1775 Hisayama residents aged ≥40 years underwent a baseline eye examination. Of those, 1401 subjects (78.9%) took part in the follow-up eye examination in 2007 and were enrolled in the present study.

Methods: At both time points, the characteristics of AMD were determined by grading color fundus photographs using the Wisconsin Age-Related Maculopathy Grading System.

Main Outcome Measures: Incident early and late AMD.

Results: The age-standardized, 9-year cumulative incidence of early AMD was 10.0%, and that of late AMD was 1.4%. Men were found to have a significantly higher incidence of late AMD than women (age-adjusted odds ratio [OR], 2.97; 95% confidence interval [CI], 1.25–7.09). The incidence of both early and late AMD increased significantly with age. Multiple logistic regression analysis showed that older age (per 1 year; OR, 1.10; 95% CI, 1.05–1.16), smoking habits (OR, 3.98; 95% CI, 1.07–14.7), and higher circulating white blood cell (WBC) count (per 1000 cells/mm^3) (OR, 1.38; 95% CI, 1.07–1.79) were significantly associated with the development of late AMD.

Conclusions: Our findings suggest that the 9-year incidences of late AMD are lower among the Japanese than among white people in Western countries, and it is higher than among black people. Smoking habits and higher circulating WBC count are significant risk factors for the development of late AMD in the Japanese.

Financial Disclosure(s): The author(s) have no proprietary or commercial interest in any materials discussed in this article. *Ophthalmology 2009;116:2135–2140 © 2009 by the American Academy of Ophthalmology.*

Age-related macular degeneration (AMD) is the leading cause of irreversible visual impairment and blindness in elderly populations in developed countries.[1] Despite the magnitude of this problem, the pathogenesis of AMD remains poorly understood. It is thus very important to determine the precise incidence of AMD and to identify its risk factors to develop preventive measures of the disease. To date, several population-based studies[2–7] including ours[8] have provided valuable information on incidence and risk factors for AMD. The risk factors examined include iris color,[2] hypertension,[3] atherosclerosis,[4] smoking habits,[5,8] higher total/high-density lipoprotein ratio,[6] and higher white blood cell (WBC) count.[7] However, information on the long-term risk of AMD is scarce[9–11] and nonexistent in Asians including Japanese.

The aim of this article was to examine the 9-year incidence of early and late AMD and its risk factors in a prospective study of a general Japanese population.

Materials and Methods

Study Population

The Hisayama Study is an ongoing, long-term, cohort study on cardiovascular disease and its risk factors in the town of Hisayama adjoining Fukuoka City, a metropolitan area in southern Japan.[12] As a part of the study, a follow-up survey of eye diseases among residents of the town has been underway.[8,13] In 1998, a total of 1775 individuals (688 men and 1775 women) aged ≥40 years underwent a baseline eye examination. Of those, 1404 subjects (79.1%) took part in the follow-up eye examination in 2007. After excluding 3 subjects who had ungradable photographs of either eye, 1401 (78.9% of the original cohort) were enrolled in the present study.

Ophthalmic Examination and Definition of Age-related Maculopathy

The methods used for the baseline eye examination have been described in detail previously.[13] Briefly, each participant under-

ISSN 0161-6420/09/$–see front matter
doi:10.1016/j.ophtha.2009.04.017

went ophthalmic examination after pupil dilatation with 1.0% tropicamide and 10% phenylephrine. Fundus photographs (45°) were taken using a Topcon TRC NW-5 fundus camera (Topcon Corporation, Tokyo, Japan), and the 35-mm color transparencies were made using Fujichrome slide film (Sensia II; Fujifilm, Tokyo, Japan). At the 9-year follow-up eye examination, fundus photographs (45°) were taken using a Topcon digital TRC NW-6SF fundus camera (Topcon Corporation). Photographs were taken of 1 field per eye.

Both examinations used a similar, masked photographic grading technique based on the International Age-related Maculopathy Epidemiological Study Group grading protocol and the grids of the Wisconsin Age-related Maculopathy Grading System.[14,15] The Wisconsin Age-related Maculopathy Grading System grid was adapted to the magnification of the camera. This protocol divides AMD into early and late stages. Early-stage AMD was defined by the presence of large drusen (soft distinct and soft indistinct) or retinal pigment epithelium pigmentary abnormalities (hyperpigmentation or hypopigmentation),[15] within the grid in the absence of late AMD in either eye. Late-stage AMD was defined as the presence of neovascular AMD or geographic atrophy. Neovascular AMD included serous or hemorrhagic detachment of the retinal pigment epithelium or sensory retina, and the presence of subretinal or subretinal pigment epithelium hemorrhages or subretinal fibrous scar tissue.[15] Geographic atrophy was characterized by sharply edged, roughly round, or oval areas of retinal pigment epithelium hypopigmentation, with clearly visible choroidal vessels.[15] The minimum area of geographic atrophy was a circle ≥175 μm in diameter. In our study, 2 experienced graders (MY, TI), masked to the subject information, assessed the AMD. Interobserver and intraobserver variability were analyzed. The level of agreement between the graders was 0.80 and 0.86 for most features. Finally, we determined the final diagnosis for disagreement cases after discussion.

Data Collection

Blood pressure was measured 3 times after the subject had rested for ≥5 minutes in the sitting position. The average of the 3 measurements was used for the analysis. Hypertension was defined as systolic blood pressure ≥140 mmHg, diastolic blood pressure ≥90 mmHg, or current use of antihypertensive medication. Blood samples were collected from an antecubital vein after an overnight fast of ≥12 hours. After taking the fasting blood specimen, a 75-g oral glucose tolerance test was performed with a 75-g glucose equivalent carbohydrate load (Trelan G; Shimizu Pharmaceutical Inc., Shimizu, Japan). Diabetes was defined as a fasting plasma glucose level ≥7.0 mmol/L, a 2-hour postloading glucose level ≥11.1 mmol/L, or a medical history of diabetes. Serum total cholesterol, high-density lipoprotein cholesterol, and triglyceride levels were determined enzymatically using an autoanalyzer (TBA-80S; Toshiba Inc., Tokyo, Japan), and dyslipidemia was defined as a total cholesterol level ≥5.7 mmol/L, high-density lipoprotein cholesterol <1.0 mmol/L, serum triglyceride level ≥1.7 mmol/L, or the current use of antihyperlipidemic medication. The WBC counts were determined using a Coulter counter (STKS; Beckman Coulter Inc., Fullerton, CA). Information on smoking habits and alcohol intake was obtained using a standard questionnaire by trained interviewers at the initial examination. Subjects were classified as either current or past habitual use or as nonuser. Body height and weight were measured in light clothing without shoes, and the body mass index (kg/m^2) was calculated.

Statistical Methods

We calculated the 9-year incidences of AMD. Age-adjusted cumulative incidences of AMD were calculated by means of the direct method using the World Health Organization standard population in 1998. Incident early AMD was defined by the appearance at follow-up of either soft drusen or retinal pigmentary abnormalities in either eye of persons in whom no early or late AMD was present at baseline. Incident late AMD was defined by the development at follow-up of neovascular AMD or geographic atrophy in either eye of persons in whom no late AMD was present at baseline. We examined the relationships between risk factors at baseline and the incidence of early and late AMD. We considered the following 9 possible risk factors for AMD: age, gender, hypertension, diabetes, dyslipidemia, smoking habits, alcohol intake, body mass index, and WBC count. Age, body mass index, and WBC count were treated as continuous variables and the others as categorical variables. Each categorical variable was coded as either 1 or 0 depending on the presence or absence of the factor, respectively. Mean values were compared by the Student *t* test, and frequencies by the chi-square test. We estimated the age-adjusted and multivariate odds ratio (OR) and 95% confidence interval (CI) of each potential risk factor by using a logistic regression analysis. The SAS software package (SAS Inc, Cary, NC) was used to perform the statistical analyses. A 2-sided *P* value of less than 0.05 was considered statistically significant.

Ethical Considerations

This study was approved by the Human Ethics Review Committee of Kyushu University Graduate School of Medical Sciences, and was carried out in accordance with the Declaration of Helsinki. Informed consent was obtained from all participants.

Results

Table 1 shows the mean values or frequencies of potential risk factors for AMD at baseline by gender. Men were older than women. The frequencies of early AMD, hypertension, diabetes, smoking habits, and alcohol intake, and mean WBC count were higher for men than for women, whereas women had the higher frequency of dyslipidemia. There was no difference in mean body mass index between the genders.

The age-adjusted, 9-year, cumulative incidences of early and late AMD lesions are shown by gender in Table 2. After excluding

Table 1. Mean Values or Frequencies of Potential Risk Factors for Age-related Macular Degeneration (AMD) by Gender at Baseline: The Hisayama Study, 1998 Early AMD and late AMD are Prevalence

Variables	Men	Women
n	524	877
Age (y), means ± SD	61±10	59±10
Early AMD (%)	18.7	11.6
Late AMD (%)	1.3	0.3
Hypertension (%)	49.4	37.6
Diabetes (%)	16.6	6.6
Dyslipidemia (%)	46.4	54.1
Body mass index (kg/m^2)	23.4±2.9	23.1±3.4
Smoking habits (%)	74.8	7.1
Alcohol intake (%)	69.1	19.6
White blood cells (×10^3/mm^3)	6.2±1.6	5.4±1.3

Table 2. Age-Standardized 9-Year Cumulative Incidences of Early and Late Age-related Macular Degeneration (AMD) by Gender: The Hisayama Study, 1998–2007

	Men		Women		All Subjects	
	Population at Risk	*Age- standardized† Incidence, n (%)*	*Population at Risk*	*Age- standardized† Incidence, n (%)*	*Population at Risk*	*Age- standardized† Incidence, n (%)*
Early AMD	426	50 (9.0)	775	93 (10.4)	1201	143 (10.0)
Pigmentary abnormalities	426	17 (3.3)	775	9 (1.3)*	1201	26 (2.0)
Soft distinct and indistinct drusen	426	33 (5.7)	775	84 (8.8)*	1201	117 (8.0)
Late AMD	517	15 (2.6)	874	8 (0.8)*	1391	23 (1.4)
Geographic atrophy	517	1 (0.1)	874	0 (0.0)	1391	1 (0.04)
Neovascular AMD	517	14 (2.5)	874	8 (0.8)*	1391	22 (1.4)

*$P<0.05$, men vs women.
†The incidence was standardized for age with the World Health Organization standard population.

190 participants with early AMD and 10 participants with late AMD at the baseline eye examination, a total of 143 participants (10.0%) developed incident early AMD during the follow-up. The incidence of early AMD was slightly but not significantly higher in women than in men. In regard to subtype of early AMD, the incidence of retinal pigmentary abnormalities was significantly higher in men than in women, whereas the incidence of drusen was significantly higher among women. After excluding 10 participants with late AMD at the baseline eye examination, a total of 23 participants (1.4%) developed late AMD during the follow-up. The incidence of late AMD was significantly higher in men than in women (age-adjusted OR, 2.97; 95% CI, 1.25–7.09) owing mainly to the significantly higher incidence of neovascular AMD in men.

Figure 1 demonstrates the age-specific incidences of early and late AMD by gender. The incidences of early and late AMD significantly increased with advancing age in both genders. In each age group, the incidence of early AMD was consistently higher in women than in men, whereas the incidence of late AMD was higher in men in age groups of ≥50 years.

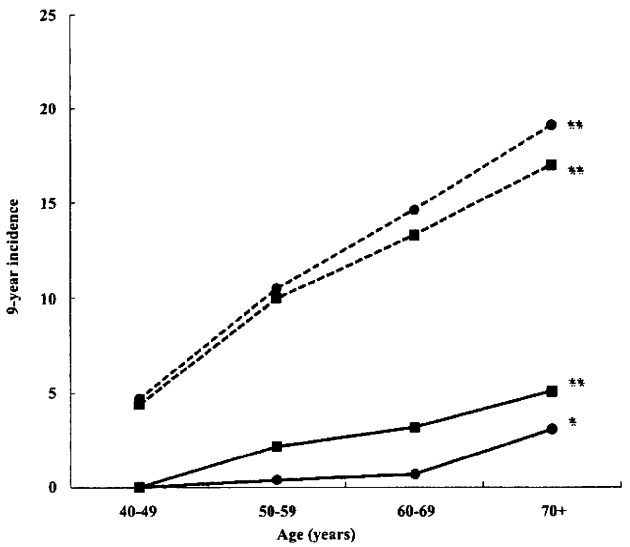

Figure 1. Age-specific 9-year incidences of early and late age-related macular degeneration by gender, the Hisayama Study. Broken line, early age-related macular degeneration; solid line, late age-related macular degeneration; black squares, men; black circles, women **$P<0.01$; *$P<0.05$ for trend.

Table 3 presents the age-adjusted, 9-year incidence of late AMD by presence or absence of early AMD at baseline. Progression to late AMD was approximately 4.4% among persons with early AMD and 0.7% among persons without early AMD. Progression to neovascular AMD was 1.8% among persons with pigmentary abnormalities and was 5.2% among persons with soft distinct and indistinct drusen. Overall, eyes with drusen at baseline were more likely to develop neovascular AMD.

The results of age- and multivariate-adjusted logistic regression analyses of risk factors for the development of early and late AMD are shown in Table 4. After adjusting for age, no associations were found between these risk factors and incident early AMD; however, male gender, smoking habits, and higher WBC count were significant risk factors for the development of late AMD. In multivariate analysis, older age, smoking habits, and higher WBC count were significantly associated with late AMD.

Discussion

To our knowledge, this is the first population-based cohort study to investigate the long-term incidence and risk factors for AMD in Japan. The findings showed that the overall, 9-year, cumulative incidence of early AMD was 10.0%, and that of late AMD was 1.4%. Both incidences increased with advancing age. Progression to late AMD was approximately 4.4% among persons with early AMD. On multivariate analysis, smoking and higher circulating WBC count were independently associated with the development of late AMD.

Previously, several long-term, population-based studies estimated the incidence of AMD. It is reported that the 10-year cumulative incidence of early AMD was 12.1% in the Beaver Dam Eye Study in the United States[9] and 14.1% in the Blue Mountains Eye Study in Australia,[11] both of which focused on a white population. The Barbados Eye Study of the predominantly black population of African descent reported a 9-year incidence of early AMD of 12.6%.[16] Even when accounting for the 1-year shorter follow-up period, our 9-year incidence of early AMD seemed to be somewhat lower than that reported in the Beaver Dam Eye Study or the Blue Mountains Eye Study. The 9-year incidence of early AMD we found (10.0%) was also lower than that reported in the Barbados Eye Study performed in a black population. Early AMD is less com-

Table 3. Age-standardized 9-Year Incidences of Late Age-related Macular Degeneration (AMD) by Presence or Absence of Early AMD at Baseline: The Hisayama Study, 1998–2007

	Geographic Atrophy		Neovascular AMD		Any Late AMD	
	Population at Risk	*Age-standardize* Incidence, n (%)*	*Population at Risk*	*Age-standardized* Incidence, n (%)*	*Population at Risk*	*Age-standardized* Incidence, n (%)*
Early AMD (−)	1,191	0 (0.0)	1,191	12 (0.7)	1,191	12 (0.7)
Early AMD (+)	190	1 (0.3)	190	10 (3.9)	190	11 (4.4)
Pigmentary abnormalities	69	1 (1.7)	69	2 (1.8)	69	3 (2.2)
Soft distinct and indistinct drusen	121	0 (0.0)	121	8 (5.2)	121	8 (5.2)

*The incidence was standardized for age with the World Health Organization standard population.

mon among the Japanese population than among white people and black people in Western countries. This difference in the incidence of early AMD among these studies could be due to the differences in study participants' characteristics (e.g., age and proportion of gender among studies), to dietary factors, to genetic factors, or perhaps to the differences in methodology among these studies.

The incidence of late AMD we found (1.4%) was lower than that reported in studies performed in white populations (Beaver Dam Eye Study, 2.1%[9]; Blue Mountains Eye Study, 3.7 %[11]) but was higher than that found in the Barbados Eye Study (0.7%), which focused on a black population.[16] This suggests that late AMD is less common among the Japanese compared with white people, and it is more common among the Japanese compared with black people. Some studies have reported racial differences in the prevalence and incidence of AMD.[17,18] The reason for different incidences among different races is not clear. However, the lower risk of occurrence of late AMD in black population was previously postulated to reflect a protective effect of melanin.[19] Weiter et al[20] have also reported that increased ocular pigmentation (iris color and fundus pigmentation) tends to decrease the risk of developing AMD, whereas Friedman et al[17] speculated that white people are genetically predisposed to have more severe maculopathy. Racial difference in late AMD incidence among the cohort studies including ours could be due to the differences in ocular pigmentation, or perhaps to genetic factors.

In the current study, the 9-year incidence of neovascular AMD was 1.4%, and that of geographic atrophy was 0.04%; nearly all incident late AMD cases were neovascular AMD (n = 22), and there was only 1 case of incident geographic atrophy. In contrast, the Blue Mountains Eye Study has reported that the 10-year incidence of neovascular AMD was 2.2%, and that of geographic atrophy was 1.7%. The incidence of geographic atrophy we found was much lower than that reported in the Blue Mountains Eye Study. The lower prevalence rates of geographic atrophy were also observed in our previous study[8] and in another Japanese population survey.[21] The reason for this different incidence, especially of geographic atrophy between Japanese and white population, is not clear. It could be due to the differences in environmental exposure or genetic factors among races.

The current study found that the incidence of early and late AMD significantly increased with advancing age in both genders. The etiology and pathogenesis of AMD are largely unknown. The consistent association with increasing age found in this study corroborated findings from many

Table 4. Age- and Multivariate-Adjusted Odds Ratios of Risk Factors for the Development of Early and Late Age-related Macular Degeneration (AMD): The Hisayama Study, 1998–2007

	Early AMD		Late AMD			
	Age Adjusted		*Age Adjusted*		*Multivariate Adjusted*	
Risk factor	*OR*	*95% CI*	*OR*	*95% CI*	*OR*	*95% CI*
Age (per 1 year)					1.10**	1.05–1.16
Gender (male)	0.92	0.63–1.33	2.97*	1.25–7.09	0.86	0.24–3.05
Hypertension	0.85	0.59–1.24	0.79	0.34–1.86		
Diabetes	0.70	0.37–1.31	0.68	0.16–2.95		
Dyslipidemia	0.92	0.65–1.31	1.32	0.56–3.08		
Body mass index (per 1 kg/m^2)	1.01	0.95–1.07	1.01	0.88–1.15		
Smoking habits	1.07	0.73–1.55	4.59**	1.86–11.3	3.98*	1.07–14.7
Alcohol intake	1.04	0.72–1.50	1.88	0.81–4.36		
White blood cells (per 10^3/mm^3)	1.03	0.91–1.16	1.52**	1.19–1.95	1.38*	1.07–1.79

CI, confidence interval; OR, odds ratio.
Multivariate adjustment was made for age, gender, smoking habit, and white blood cells.
*P<0.05; **P<0.01.

other studies,[9,11,16] confirming the age-related nature of the disease.

We found a significantly higher incidence of late AMD in men than in women. We have already reported that early and late AMD were more prevalent among men than women in a cross-sectional study of Hisayama residents.[13] A similar finding was also observed in another cross-sectional study in Japan.[21] In contrast, most studies conducted in Western, white populations have shown a higher prevalence of late AMD in women.[11,22] The reason for this difference is precisely unknown, but smoking habits, which are known to be a major risk factor for AMD,[7,22,23] are likely to contribute to a higher incidence of late AMD in Japanese men, because the proportion of habitual smoking is much higher for men than women in Japan.

The results of this study provide prospective evidence that cigarette smoking increases the risk of developing late AMD. Compared with those who never smoked, those who had smoked in the past or were currently smoking had approximately a 4.0 times higher risk of late AMD, after adjusting for other potential risk factors. These findings are consistent with other cross-sectional and cohort data, which showed that cigarette smoking was related to the development of late AMD.[7,22,23] Smoking habits remain highly prevalent among Japanese men (74.8% in our men), which translates to a 73.8% of population-attributable fraction for late AMD in our men that are attributable to their smoking behavior. Because smoking is a well-recognized, modifiable risk factor for AMD, smoking cessation is an important public health measure to reduce the burden of AMD, particularly among Japanese men.

We found that a higher WBC count was associated with incident late AMD, independent of age, gender, and smoking status. A similar association was also observed in the Blue Mountains Eye Study.[7] Several recent experimental evidences suggest that the association between higher WBC count and late AMD is plausible, including the role of inflammatory mechanisms in subretinal neovascularization[24] and drusen development.[25] Chronic inflammatory cells, including macrophage leukocytes, have been observed in excised neovascular membranes from patients with late AMD.[26] Ultrastructural study on subretinal neovascularization associated with late AMD suggested that activated WBC are involved in the promotion of neovascular proliferation and exudation from new vessels.[24] These findings provide important evidence of an essential link between inflammation and late AMD development and suggest that local inflammatory processes that have long been known to be associated with subretinal neovascularization and drusen development may be reflected in the systemic inflammatory marker of higher WBC count.

This study has several limitations. First, losses to follow-up, an issue inherent to all long-term cohort studies, could have introduced selection bias, resulting in either an underestimation or overestimation of AMD incidence. Second, the early AMD definition used in this study is less strict and includes more early AMD cases than the definitions used by the Beaver Dam[11] and the Blue Mountains[13] Eye Studies: Drusen were defined as either indistinct or distinct drusen in our study, whereas they were defined as indistinct soft drusen in the abovementioned studies. If this study used the same early AMD definition used in other 2 studies, the early AMD incidence could have been lower than the currently reported 10%.

In conclusion, the results of this study suggest that early and late AMD is less common among the Japanese compared with white people in Western countries, although late AMD is more common among the Japanese compared with black people, and that older age, smoking habits and higher WBC count are relevant risk factors for late AMD in the Japanese. This finding provides important epidemiologic evidence of an essential link between inflammation and late AMD development, and also support the use of anti-inflammatory agents in the treatment of late AMD.

References

1. Munoz B, West SK, Rubin BS, et al, SEE Study Team. Causes of blindness and visual impairment in a population of older Americans: the Salisbury Eye Evaluation Study. Arch Ophthalmol 2000;118:819–25.
2. Mitchell P, Smith W, Wang JJ. Iris color, skin sun sensitivity, and age-related maculopathy: the Blue Mountains Eye Study. Ophthalmology 1998;105:1359–63.
3. Sperduto RD, Hiller R. Systemic hypertension and age-related maculopathy in the Framingham Study. Arch Ophthalmol 1986;104:216–9.
4. Vingerling JR, Dielemans I, Bots ML, et al. Age-related macular degeneration is associated with atherosclerosis: the Rotterdam Study. Am J Epidemiol 1995;142:404–9.
5. Klein R, Klein BE, Linton KL, DeMets DL. The Beaver Dam Eye Study: the relation of age-related maculopathy to smoking. Am J Epidemiol 1993;137:190–200.
6. Tan JS, Mitchell P, Smith W, Wang JJ. Cardiovascular risk factors and the long-term incidence of age-related macular degeneration. Ophthalmology 2007;114:1143–50.
7. Shankar A, Mitchell P, Rochtchina E, et al. Association between circulating white blood cell count and long-term incidence of age-related macular degeneration: the Blue Mountains Eye Study. Am J Epidemiol 2006;165:375–82.
8. Miyazaki M, Kiyohara Y, Yoshida A, et al. The 5-year incidence and risk factors for age-related maculopathy in a general Japanese population: the Hisayama Study. Invest Ophthalmol Vis Sci 2005;46:1907–10.
9. Klein R, Klein BE, Tomany SC, et al. Ten-year incidence and progression of age-related maculopathy: the Beaver Dam Eye Study. Ophthalmology 2002;109:1767–79.
10. Klein R, Klein BE, Knudtson MD, et al. Fifteen-year cumulative incidence of age-related macular degeneration: the Beaver Dam Eye Study. Ophthalmology 2007;114:253–62.
11. Wang JJ, Rochtchina E, Lee A, et al. Ten-year incidence and progression of age-related maculopathy: the Blue Mountains Eye Study. Ophthalmology 2007;114:92–8.
12. Katsuki S. Epidemiological and clinicopathological study on cerebrovascular disease in Japan. Prog Brain Res 1996;21: 64–89.
13. Miyazaki M, Nakamura H, Kubo M, et al. Risk factors for age related maculopathy in a Japanese population: the Hisayama Study. Br J Ophthalmol 2003;87:469–72.
14. Bird AC, Bressler NM, Bressler SB, et al, International ARM Epidemiological Study Group. An international classification and grading system for age-related maculopathy and age-